NOTE TO USERS

Performance Analysis of WCDMA Downlink Systems with Antenna Array

Meiyu Qin

A Thesis

in

The Department

of

Electrical and Computer Engineering

Presented in Partial Fulfillment of the Requirements
For the Degree of Master of Applied Science at
Concordia University,
Montreal, Quebec, Canada

April 2005

Your file Votre référence
ISBN: 0-494-04389-X
Our file Notre référence
ISBN: 0-494-04389-X

ABSTRACT

Performance Analysis of WCDMA Downlink Systems with Antenna Array

Meiyu Qin

Wide-band code division multiple access (WCDMA) is considered one of the best multiple access techniques for the third-generation (3G) wireless communication systems due to its spectral efficiency compared to other schemes. Chosen by UMTS (Universal Mobile Telecommunications System), the WCDMA technique has received increasing research interest in recent years. As the 3G and 4G communication systems aim to provide mobile users with flexible high-speed multimedia services, such as high quality image and video, the data traffic in the downlink channel will be much higher than in the uplink channel. This thesis focuses on the performance study of WCDMA downlink systems that use antenna array receivers.

The work of the thesis begins with a study of the physical layer tasks of WCDMA systems, including some key techniques and channel structures for both downlink and uplink with an emphasis on the downlink common pilot channel and the time-multiplexed pilot symbol structure. Multipath fading effects and Rake receiver techniques are also

covered. These techniques and channel configurations are then used for the simulation of the entire WCDMA downlink system.

The second part of this thesis is concerned with antenna array processing techniques and the performance of a two-element antenna that can easily be incorporated into mobile handsets. A simulation study of an antenna array receiver is carried out for various parameters and different combining schemes. The main contribution of the thesis is in the investigation of the downlink performance of a WCDMA system using an adaptive antenna array. Both temporal and spatial diversities are taken into account in the simulation. Based on the WCDMA specification, it is found that the spatial-temporal receiver with $\lambda/4$ (3.5cm) distance between the antenna elements can provide strong beamforming capability. The diversity gain of a smart antenna system with different combining schemes is also examined. It is shown that when both spatial and temporal signal processing techniques are combined, the multiple access interference and the multipath fading effect can be significantly mitigated or eliminated.

ACKNOWLEDGEMENTS

I would like to express my sincere gratitude to my research advisor and thesis supervisor, Dr. Wei-Ping Zhu, for supporting and providing me an opportunity to pursue research in WCDMA wireless communication field, and for providing me with continuous feedback and encouragement during the completion of the thesis work. His suggestions and advices have allowed me to overcome the difficult times during my study. I am truly grateful for his invaluable insights and confidence during the course of this work.

I am also grateful to all the professors with whom I have interacted during my studies at Concordia University. And I would like to thank all my friends in Concordia University. It has been a great pleasure studying and working with them.

Finally, I would like to express my heartfelt appreciations to my family. Their unconditional love and encouragement accompany with me throughout all these years.

I dedicate this work to my father .....

Contents

LIST OF TABLES

LIST OF FIGURES

LIST OF ABBREVIATIONS AND SYMBOLS

AC	Adaptive Combining
3GPP	Third-Generation Partnership Project
AWGN	Additive White Gaussian Noise
BER	Bit Error Rate
BPSK	Binary Phase-Shift Keying
CDMA	Code Division Multiple Access
CPICH	Common Pilot Channel
DPCH	Dedicated Physical Channel
DPCCH	Dedicated Physical Control Channel
DPDCH	Dedicated Physical Data Channel
DOA	Direction of Arrival
DS	Direct-Sequence
DS-CDMA	Direct-Sequence Code Division Multiple Access
ETSI	European Telecommunications Standards Institute
FDD	Frequency Division Duplex
FDMA	Frequency Division Multiple Access
GPRS	General Packet Radio Services
IMT	International Mobile Telecommunications
ITU	International Telecommunication Union

LES	Linear Equally Spaced
LMS	Least Mean Squared
MAI	Multiple Access Interference
MRC	Maximal Ratio Combining
MMSE	Minimum Mean Square Error
MSE	Mean Square Error
OVSF	Orthogonal Variable Spreading Factor
PN	Pseudo Random Noise
QPSK	Quadrature Phase Shift Keying
SA	Single Antenna
SINR	Signal-to-Interference-plus-Noise Ratio
SNOI	Signal-Not-Of-Interest
SNR	Signal -to-Noise Ratio
SOI	Signal-Of-Interest
STR	Space-Time Receiver
TDD	Time Division Duplex
TDMA	Time Division Multiple Access
UMTS	Universal Mobile Telecommunication System
UTRA	Universal Terrestrial Radio Access
WCDMA	Wideband Code Division Multiple Access
WLAN	Wireless Local Area Network

$b(t)$	Information signal
c	Light speed
C_K	OVSF code for user k
d	The distance between the antenna elements
$E[\cdot]$	Expected value of a random variable
$F(\Phi)$	Matrix of the steering vectors
e	Error signal
f_c	Carrier frequency
f_m	Maximum Doppler frequency
$G(\Phi)$	Antenna array response
$I(t)$	Interference
$J(w)$	Cost function
$n(t)$	Additive white Gaussian Noise
$\mathbf{P}$	Cross correlation matrix of the input signal and the desired signal
$r(\cdot)$	Received signal at the receiver
$r_l(\cdot)$	Received l^{th} path signal
$\mathbf{R}$	The correlation matrix of the input data vector
$s(t)$	Baseband complex envelope
S_{DL}	Scrambling code for the signal
$SF-Data$	Spreading factor of the data
$SF-CPICH$	Spreading factor of the Common Pilot Channel

T_c	Chip duration of the spreading sequence
T_s	Symbol period
v	Velocity of the mobile relative to the base station
$\mathbf{w}$	Filter coefficient vector with length P
$\mathbf{w}_{opt}$	Optimal weight in the MMSE sense
y_k	The output of the k^{th} user's correlator
α_m	The complex gain of m^{th} path
$\delta(\cdot)$	Delta function
λ	Wavelength of the carrier waveform
μ	Step-size
σ^2	Variance of Gaussian noise
τ_k	Time delay of the k^{th} signal to the array reference element
θ, φ	The arrival angle of the signal,
$\Re\{\cdot\}$	Real part of $\{\cdot\}$
$(\cdot)^*$	Complex conjugate
$(\cdot)^H$	Complex conjugate transpose
∇	Gradient of a function

Chapter 1

Introduction

1.1 Third-Generation Mobile Communication Systems

Unlike the first generation wireless communication systems which are basically analog cellular systems dedicated to voice communication, the second generation systems which are the digital systems currently in use, such as GSM, PDC, CDMA-I (IS-95) and US-TDMA (IS-136) [1]-[3], have been designed to provide both voice and data services. The third-generation (3G) systems [4]-[6] are now being developed for multimedia telecommunications in order to meet the increasing demand of wideband services. The 3G mobile communication systems must be designed to comply with a global standard that supports a high degree of commonality, seamless roaming, a high spectral efficiency, and a variety of voice and data services for both mobile and fixed users. Many of these features are already fulfilled by the second-generation systems. However, the major services provided by these systems are limited to voice, facsimile, and low bit rate data. The 3G systems aim to provide customers with a variety of versatile broadband services, from multimedia to interactive and universal services. The state of the art person-to-person communication should provide flexible communication services with high quality image and video. These service expectation and objectives of future mobile

wireless standards have been clearly defined in the International Telecommunication Union (ITU) IMT-2000 standard [7]. The ITU is the international body responsible for allocating international telecommunication frequencies and its IMT-2000 standard is the globally accepted standard for 3G wireless communications. IMT-2000 provides "a framework for worldwide wireless access by linking the diverse systems of terrestrial and/or satellite-based networks". It is in this IMT-2000 document that ITU sketches out a vision for all future 3G mobile wireless standards including its main objectives summarized below:

- Improved system capacity;
- Backward compatibility with second-generation(2G) systems;
- Multimedia support; and
- High speed packet data services.

Despite some limitations, the CDMA (Code Division Multiple Access) technique is considered the best multiple access technique available as it makes the most efficient use of the radio frequency spectrum in comparison to other schemes.

Wideband CDMA (WCDMA) and CDMA2000 are currently being considered as two major air interface standards to be adopted for 3G telecommunication systems. Both of them meet the International Telecommunication Union (ITU) International Mobile Telecommunications (IMT)-2000 requirements. ETSI (European Telecommunications Standards Institute) has chosen the WCDMA technology as basic radio-access technology for the UMTS (Universal Mobile Telecommunications System). The goal of UMTS is to

enable networks to offer true global roaming and support a wide range of voice, data and multimedia services.

The WCDMA specification has been created in the Third Generation Partnership Project (3GPP) which was proposed by Europe and Japan. It is designed to be backward compatible with the Global System for Mobile communication (GSM) system, which is a second generation TDMA standard employed mainly in Europe. The CDMA2000 system proposed by Telecommunications Industry Association (TIA) is evolved from IS-95 which is a second generation CDMA standard adopted in North America and Korea.

The new UMTS network will be built on the success of GSM and its operators' existing investments in infrastructure. The first stage of the service and network evolution is from today's GSM system, through the implementation of GPRS (General Packet Radio Services), to commercial UMTS networks. Many of the original goals of UMTS are being met by the evolving GSM standard such as global roaming and personalized service features. The major difference between UMTS and GSM is in the new air interface operating at around 2GHz which will offer superior performance to GSM in terms of data rate and capacity. UMTS will offer a data rate of 144 kb/s in wide-area mobile environments, 384 kb/s in vehicular, pedestrian and urban environments, or 2Mb/s in fixed and in-building environments [9].

Spread spectrum techniques have been established for antijam, multipath rejection, accurate ranging and tracking applications. The direct sequence CDMA (DS-CDMA) based upon spread spectrum techniques has been successfully used in the

second-generation systems such as IS-95 to support mobile communications. The analytical and simulation results indicate that for terrestrial telephony, the interference suppression using the DS-CDMA technique can result in a significant increase in capacity over other technologies such as TDMA and FDMA. This has led to a popular adoption of DS-CDMA as a major wireless access technique for most of the air interface standards (WCDMA, CDMA2000) for 3G systems. The advantages of the DS-CDMA technique include the single frequency reuse, enhancement of transmission performance via diversity techniques such as Rake combining and antenna array, and a direct capacity increase by use of sectored antennas, handoff, and power control. The new capabilities that can be used to enhance the performance of 3G systems can be summarized as follows:

- Broader bandwidth and higher chip rate
- Provision of multi-rate services
- Coherent detection using dedicated pilot
- Fast power control for uplink/downlink
- Packet Data transmission
- Optional Multi-user Detection

1.2 Motivation

Since a WCDMA system is aimed to provide mobile users with high-speed multimedia communication services including wireless Internet, video-on-demand and

other multimedia applications, data traffic in the downlink channel will be much higher than in the uplink channel. An efficient implementation of downlink receivers is therefore of crucial importance in the development of WCDMA systems. However, the downlink capacity is limited by both multipath fading and Multiple-Access Interference (MAI).

The code orthogonality in CDMA based systems is often destroyed by multipath fading and therefore, needs to be restored or at least mitigated prior to symbol detection. Besides, the interfering signals from neighboring base stations have to be taken into account for optimum reception performance. To improve signal reception at mobile terminals, various Transmit Diversity (TD) schemes have been proposed to mitigate the performance degradation due to multipath fading. Some advanced receiver techniques such as multiuser detection and smart adaptive antennas [11] may also be needed in mobile terminals.

Previous research on mobile communication systems indicates that the addition of adaptive circuitry can overcome most of the system impairments caused by the effects of multipath fading. Although antenna diversity techniques are nowadays by default employed in the base station, the additional cost and complexity as well as the uncertainty in performance enhancement in terminal side have so far prevented antenna arrays from being utilized in the existing mobile systems. In wireless personal communications, the use of antenna arrays with space-time processing can provide a much higher gain in receiver's performance through mitigating the propagation distortion and interference [9]-[15].

A smart antenna not only suppresses interference, but also combats multipath fading by combining multiple antenna signals. To process multiple antenna signals, two combining schemes—diversity combining and adaptive combining—can be employed. Diversity combining exploits the spatial diversity among multiple antenna signals and achieves higher performance. There are four classical diversity combining schemes, switched diversity, selection diversity, equal gain combining, and maximal ratio combining (MRC) [16]-[17]. After weighting each antenna signal proportional to its Signal to Noise Ratio (SNR), MRC can provide a maximum output SNR. Adaptive combining is based on dynamic reconfiguration in that the antenna weights are dynamically adjusted to enhance the desired signal while suppressing interfering signals in order to maximize the Signal to Interference plus Noise Ratio (SINR). It achieves the same performance as the MRC without the presence of interference. The performance of adaptive combining is sometimes limited under certain circumstances, especially when the angular separation between the desired signal and the interference is small or the noise level is high [15]. Because of concerns with high system complexity and high power consumption, smart antenna techniques have been considered primarily for base station so far [18]-[23].

A common belief is that closely spaced antennas are ineffective for exploiting diversity. However, recent measurement results indicate that even closely spaced antennas (such as 15% of the wavelength) provide a low envelope correlation to yield a diversity gain [24]. Some of the on-going studies show that adaptive antennas in the

terminals could be extremely powerful in existing mobile systems. The results reported in [25] indicate that a two-antenna GSM terminal could suppress co-channel interference by 5~10 dB depending on the power of the dominant interfering signal with respect to others.

A dual-antenna system for handsets has also been investigated for the Digital European Cordless Telephone (DECT) system for indoor radio channels [26]. Also, the Third Generation Partnership Project (3GPP) requires antenna diversity at base stations and optionally at mobile terminals [4], [27]. Antenna diversity is also applied to the IEEE 802.11 Wireless Local Area Network (WLAN) system [28]. The problem of antenna fading correlation and branch power difference between closely spaced antennas in handset terminals has been addressed by some experimental studies, showing encouraging results with respect to correlation [29]-[30]. For applications in small handsets there is a severe space limitation that precludes the use of a fairly large number of sensors. On the other hand, new concepts of wearable portable devices may solve this space limitation problem, and a large number of sensors may become a reality for this application.

In this thesis, we propose a smart antenna receiver for handsets in 3G WCDMA systems. We demonstrate the effectiveness of employing the smart antenna system and compare the performance by using different adaptive combining methods.

1.3 Objective and Organization of the Thesis

The objective of this thesis is to study the performance improvement of WCDMA downlink systems from using smart antennas in mobile terminals. The performance of the proposed algorithms is evaluated with link simulator in accordance with WCDMA specifications [31]-[32], and is compared with that of some of the algorithms existing in literature.

The remainder of the thesis is organized as follows.

Chapter 2 reviews the fundamentals of WCDMA systems, including system configurations, modulation and multiplexing techniques, multipath fading channels and Rake receiver. Chapter 3 presents smart antenna techniques and relevant investigation results. The emphasis is placed on the array structure, adaptive beamforming and the adaptation of the array response vector. Some simulation results are also provided. A detailed simulation study and performance analysis of the WCDMA downlink system using antenna array are carried out in Chapter 4 under different channel conditions. Various simulation results are shown for different channel environments and adaptive combining schemes. Finally, Chapter 5 concludes the thesis by highlighting the major contributions of the completed research and gives some suggestions for future study.

Chapter 2

Fundamentals of WCDMA Systems

2.1 Introduction

As mentioned in the previous chapter, WCDMA is the technology developed for the FDD mode of the European 3G mobile communication standard – UMTS (Universal Mobile Telecommunication System). This technology is based on the Direct Sequence CDMA (DS-CDMA) principle.

In this chapter, we first briefly review the concept of spread spectrum and Code Division Multiple Access (CDMA) techniques. We then provide a physical layer description of the radio access network of a WCDMA system operating in the FDD mode and describe the frame structure of various physical channels. In Section 2.3, the spreading and modulation operations for the Dedicated Physical Channels (DPCH) at both uplink and downlink are illustrated in detail, and the spreading codes used in both links are also investigated.

The nominal bandwidth for third generation proposals is 5 MHz; this high bandwidth allows the received signal to be split into distinct multipaths with high resolution, and allows more multipaths to be resolved than narrower bandwidth. In Section 2.4, we

introduce multipath channels and Rake receiver technique.

2.2 Spread Spectrum and Code Division Multiple Access

In traditional radio communication systems, the carrier is modulated with user data using techniques that minimize the transmitted bandwidth to conserve spectrum resources. This is because these systems are designed so that only a single channel occupies a given frequency band. If signals are transmitted in multiple non-overlapping frequency bands, they do not interfere with each other and the signals may be recovered, provided that the power levels are high enough relative to the noise present in the channel. In a spread spectrum system, rather than trying to minimize the bandwidth of the modulated signal, the goal is to create a modulated signal that uses a large amount of bandwidth. In fact, spread spectrum systems (e.g., direct sequence spread spectrum using CDMA) have found applications in military systems for a long time. They use a very large bandwidth to transmit a spread signal that is generated by multiplying the information bits with a signature code or spreading sequence.

2.2.1 Code Division Multiple Access (CDMA)

A number of different multiple access schemes have been used in wireless systems. Historically, the most common multiple access techniques are Frequency Division

Multiple Access (FDMA), Time Division Multiple Access (TDMA) and CDMA. In FDMA, different channels are separated by giving each channel a unique frequency band; in TDMA, the channels are made orthogonal by separating them in time, with all users using the same frequency band; while in CDMA, all users can transmit simultaneously on the entire available bandwidth using a pseudorandom code that is unique for each user and is orthogonal to the code sequences used by other channels. These concepts are illustrated in Figure 2-1 [4], [35]. Therefore, CDMA allows many users to occupy the same time and frequency allocations in a given band. In CDMA systems, the narrow band message signal is multiplied by a large bandwidth pseudorandom noise (PN) code. The transmitted signal is then recovered by correlating the received signal with the same PN code as used by the transmitter.

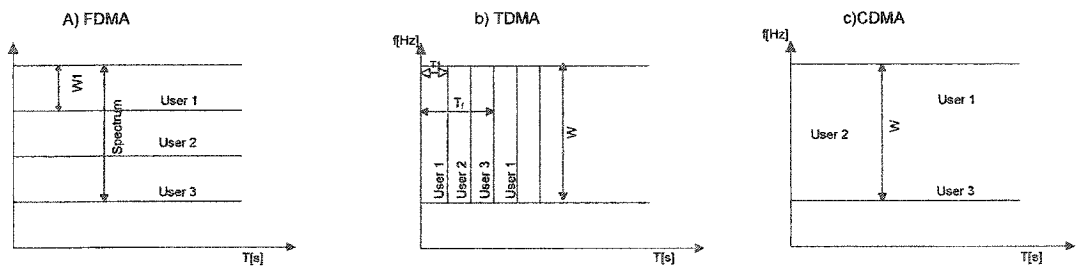

Figure 2-1: Three multiple access schemes
(a) Frequency Division Multiple Access (FDMA);
(b) Time Division Multiple Access (TDMA);
(c) Code Division Multiple Access (CDMA)

CDMA has been one of the fastest growing wireless technologies and continues to grow at a faster pace than any other technology. Many spread spectrum techniques are currently available. For the reason that WCDMA uses Direct Sequence Spread Spectrum (DS-SS) technique, only this access scheme is explained in this thesis.

2.2.2 Direct Sequence Spread Spectrum

In a direct sequence (DS) system, consider an information signal $b(t)$ which is composed of a sequence of symbols, b_j, each of duration T_s. The data signal is given by

$$b(t) = \sum_{j=-\infty}^{\infty} b_j P_{T_s}(t - jT_s) \tag{2.1}$$

where $P_{T_s}(t)$ is the pulse shape of the bit. For simplicity, here we assume a rectangular shape, namely

$$P_{T_s}(t) = \begin{cases} 1 & 0 \le t \le T_s \\ 0 & otherwise \end{cases} \tag{2.2}$$

Later in our simulation we will use a square-root raised cosine filter for pulse shaping according to the WCDMA standard. This signal is multiplied by a PN sequence C(t):

$$C(t) = \sum_{j=-\infty}^{\infty} C_j P_{T_c}(t - jT_c) \tag{2.3}$$

where C_j is the j^{th} chip of a discrete periodic PN sequence assigned to the user and takes on values of $C_j \in \{\pm 1\}$ with a duration of T_c. $P_{T_c}(t)$ has the same function as $P_{T_s}(t)$. The multiplied signal, $b(t)C(t)$, is then up-converted to a carrier frequency f_c by multiplying $b(t)C(t)$ by the carrier. Thus, the transmitted signal $s(t)$ is given by

$$s(t) = b(t)C(t)\cos(2\pi f_c t) \tag{2.4}$$

Let us assume, for the moment, that the channel does not distort the signal in any way so that the received signal, $r(t)$, consists of the transmitted signal with added white

Gaussian noise, $n(t)$.

$$r(t) = As(t) + n(t) = Ab(t)C(t)\cos(2\pi f_c t) + n(t) \tag{2.5}$$

At the receiver, a local replica of the chip sequence, $C(t-\tau_0)$, is generated, where τ_0 is a random time offset between 0 and MT_c. To de-spread the signal at the receiver, the local chip sequence must be synchronized with the received signal. This means that the timing offset, τ_0, must be set to zero. One means of doing this is through the use of a Delayed Locked Loop (DLL). Similarly, a Phase delayed Locked Loop (PLL) may be used to create a replica of the carrier $\cos(2\pi f_c t)$. Using these two quantities, a decision statistic is formed by multiplying the received signal by the local PN sequence and the local oscillator, and by integrating the result over one data symbol:

$$\begin{aligned} d_j &= \int_{jT_s}^{(j+1)T_s} r(t)C^*(t)\cos(2\pi f_c t)dt \\ &= \int_{jT_s}^{(j+1)T_s} \{Ab(t)C(t)\cos(2\pi f_c t) + n(t)\}C^*(t)\cos(2\pi f_c t)dt \end{aligned} \tag{2.6}$$

From $C(t)C^*(t) = 1$, then we have

$$\begin{aligned} d_j &= \int_{jT_s}^{(j+1)T_s} \{Ab(t)\cos^2(2\pi f_c t) + n(t)C^*(t)\cos(2\pi f_c t)\}dt \\ &= Ab_j\left(\frac{T_s}{2} + \frac{1}{2\times 4\pi f_c}(\sin(4\pi f_c(j+1)T_s) - \sin(4\pi f_c jT_s))\right) + \eta \end{aligned}$$

where η represents the influence of the channel noise on the decision statistic, and

$$\eta = \int_{jT_s}^{(j+1)T_s} n(t)C^*(t)\cos(2\pi f_c t)dt \tag{2.7}$$

Assuming that the carrier frequency is large relative to the reciprocal of the bit period,

i.e., $w_c >> 1/T_s$, then

$$d_j = \frac{Ab_jT_s}{2} + \eta \tag{2.8}$$

Therefore, the decision statistic, d_j, is an estimate, $\hat{b}_j$, of the transmitted data symbol b_j.

If the channel noise is Additive White Gaussian Noise with two-sided power spectral density $N_0/2$, then the variable η is a zero mean Gaussian random variable $\mu_n = 0$ with variance $\sigma_\eta^{\ 2} = \frac{N_0T_s}{4}$ [45].

Spread spectrum techniques have many advantages:

- Let each user is multiplied by a different orthogonal PN sequence C(t); many DS signals can be overlaid on top of each other in the same frequency.
- Since the signal is spread over a large bandwidth with the same total power, the spectral density of the signal can be very small. This makes it difficult for an eavesdropper to detect the signal. Also, if the eavesdropper does not know the PN-sequence used, it will be very difficult to extract the information.
- The fact that the DS signal is spread over a large bandwidth can significantly mitigate the effects of fading which can degrade the performance of narrowband systems. Various techniques can be used to recover the signal as long as some portion of the received signal has not faded.

2.2.3 Multiple Access Technology

2.2.3.1 Multiple Access Interference in DS-CDMA Systems

Consider a CDMA system in which K users occupy the same frequency band at the same time. These users may share the same cell, or some of the K users may communicate with other base stations.

The signal received at the base station from user k is given by

$$s_k(t-\tau_k)=\sqrt{2P_k}C_k(t-\tau_k)b_k(t-\tau_k)\cos(w_c t+\phi_k) \tag{2.9}$$

where $b_k(t)$ is the data sequence for user k, $C_k(t)$ is the spreading sequence for user k, τ_k is the delay of user k relative to a reference user 0, P_k is the corresponding received power, and ϕ_k is the phase offset of the k-th user. Since τ_k and ϕ_k are relative terms, we can define $\tau_0 = 0$ and $\phi_0 = 0$.

Let us assume that both $C_k(t)$ and $b_k(t)$ are binary sequences having values of -1 or +1. The chip sequence $C_k(t)$ is of the form

$$C_k(t)=\sum_{j=-\infty}^{\infty}\sum_{i=0}^{M-1}C_{k,i}P_{T_c}(t-(i+jM)T_c) \quad C_{k,i}\in(-1 \quad 1) \tag{2.10}$$

where M is the number of chips sent in a PN sequence period and T_c is the chip period. MT_c is the repetition period of the PN sequence.

For the data sequence $b_k(t)$, T_b is the bit period. It is assumed that the bit period is an integer multiple of the chip period, i.e., $T_b = NT_c$. Note that M and N do not need to be same. The binary data sequence $b_k(t)$ is given by

$$b_k(t) = \sum_{j=-\infty}^{\infty} b_{k,j} P_{T_b}(t - jT_b) \qquad b_{k,j} \in \{-1 \quad 1\} \tag{2.11}$$

The signal available at the input to the correlator is given by

$$r(t) = \sum_{k=0}^{K-1} s_k(t - \tau_k) + n(t) \tag{2.12}$$

where n(t) is additive Gaussian noise with two-sided power spectrum density $N_0/2$. It is assumed in (2.12) that there are no multipaths in the channel, with the possible exception of multipaths that lead to flat fading such that the coherence time of the channel is considerably larger than a symbol period [17]. At the receiver, the received signal is mixed down to baseband, multiplied by the PN sequence of the desired user (user 0 for example) and integrated over one bit period. Thus, assuming that the receiver is delay and phase synchronized with user 0, the decision statistic for user 0 is given by

$$d_0 = \int_{jT_b}^{(j+1)T_b} r(t) C_0^*(t) \cos(2\pi f_c t) dt \tag{2.13}$$

For convenience and simplicity of the notation, the remainder of the analysis is presented for the case of bit 0 (j=0 in (2.13)). Substituting (2.9) and (2.12) into equation (2.13),

$$d_0 = \int_0^{T_b} \left[\sum_{k=0}^{K-1} \sqrt{2P_k} b_k(t - \tau_k) C_k(t - \tau_k) \cos(2\pi f_c t + \phi_k) + n(t) \right] C_0^*(t) \cos(2\pi f_c t) dt \tag{2.14}$$

which may be expressed as

$$d_0 = I_0 + \eta + \zeta \tag{2.15}$$

where I_0 is the contribution to the decision statistic from the desired user(k=0), ζ is the multiple access interference, and η is the noise contribution. The contribution from

the desired user is given by

$$I_0 = \sqrt{2P_0}\int_0^{T_b} b_0(t)\left|C_0(t)\right|^2 \cos^2(2\pi f_c t)dt$$

$$= \sqrt{\frac{P_0}{2}} b_{0,0}\int_0^{T_b} (1+\cos(4\pi f_c t))dt$$

$$= \sqrt{\frac{P_0}{2}} b_{0,0} T_b \tag{2.16}$$

The noise term, η is given by

$$\eta = \int_0^{T_b} n(t)C_0^*(t)\cos(2\pi f_c t)dt \tag{2.17}$$

where it is assumed that $n(t)$ is additive Gaussian noise with two-sided power spectrum density $N_0/2$. The mean of η is

$$\mu_n = E[\eta] = \int_0^{T_b} E[n(t)]C_0^*(t)\cos(2\pi f_c t)dt = 0 \tag{2.18}$$

The third component in (2.15), ζ, represents the contribution of multiple access interference to the decision statistic, which is the summation of K-1 terms I_k,

$$\zeta = \sum_{k=1}^{K-1} I_k \tag{2.19}$$

where

$$I_k = \int_0^{T_b} \sqrt{2P_k} b_k(t-\tau_k)C_k(t-\tau_k)C_0^*(t)\cos(2\pi f_c t + \phi_k)\cos(2\pi f_c t)dt \tag{2.20}$$

Therefore, we get the received signal at the base station in detail.

2.2.3.2 WCDMA UTRA (Universal Terrestrial Radio Access) FDD/TDD Modes

The WCDMA system within 3GPP has been divided into two modes according to the

radio access technologies used: UTRA (Universal Terrestrial Radio Access) FDD (Frequency Division Duplex) and UTRA TDD (Time Division Duplex).

- FDD: The uplink and downlink transmissions employ two separate frequency bands. A pair of frequency bands with specified separation is assigned for a connection.
- TDD: In this duplex method, uplink and downlink transmissions are carried over the same frequency band by using synchronized time intervals. Thus, time slots in a physical channel are divided into transmission and reception parts.

The spectrum allocation for these two modes is as follows.

- 1920-1980 MHz: FDD Uplink
- 2110-2190 MHz: FDD Downlink
- 1900-1920 MHz: TDD
- 2020-2025 MHz: TDD

The TDD mode is based heavily on FDD mode concept and is added in order to leverage the basic WCDMA system for use with unpaired spectrum allocation for IMT-2000 systems. In this thesis, we discuss the performance of a WCDMA system operating only in the FDD mode. Next we provide a more detailed description of the physical layer of the radio access network of a WCDMA system operating in the FDD mode.

2.3 Physical Channel Structure of WCDMA Systems

WCDMA defines two dedicated physical channels in both uplink and downlink according to the usage:

- Dedicated Physical Data Channel (DPDCH): to carry dedicated data generated at layer 2 and above.
- Dedicated Physical Control Channel (DPCCH): to carry layer 1 control information.

Each connection is allocated one DPCCH and zero, one or several DPDCHs. In addition, there are common physical channels defined as:

- The Common Pilot Channel (CPICH) for coherent detection.
- Primary and secondary Common Control Physical Channels (CCPCH) to carry downlink common channels.
- Synchronization Channels (SCH) for cell search.
- Physical Random Access Channel (PRACH).

In the physical layers, the WCDMA system employs a frame structure [31]. Each frame lasts 10ms and it is split into 15 slots. The chip rate is 3.84Mcps which corresponds to 2560 chips per slot. The data rate is dependent on the spreading factor, which varies in powers of 2 from 256 to 4 in the uplink and from 512 to 4 in the downlink. For example, if the channel uses a spreading factor of 16, then the bit rate is 480 Kbps ((3.84Mbps/16)× 2). Therefore, the bit rate varies from 30 Kbps to 1920 Kbps in uplink

and from 15 Kbps to 1920 Kbps in downlink.

2.3.1 Uplink Physical Channels

Figure 2-2 shows the principal frame structure of the uplink dedicated physical channels.

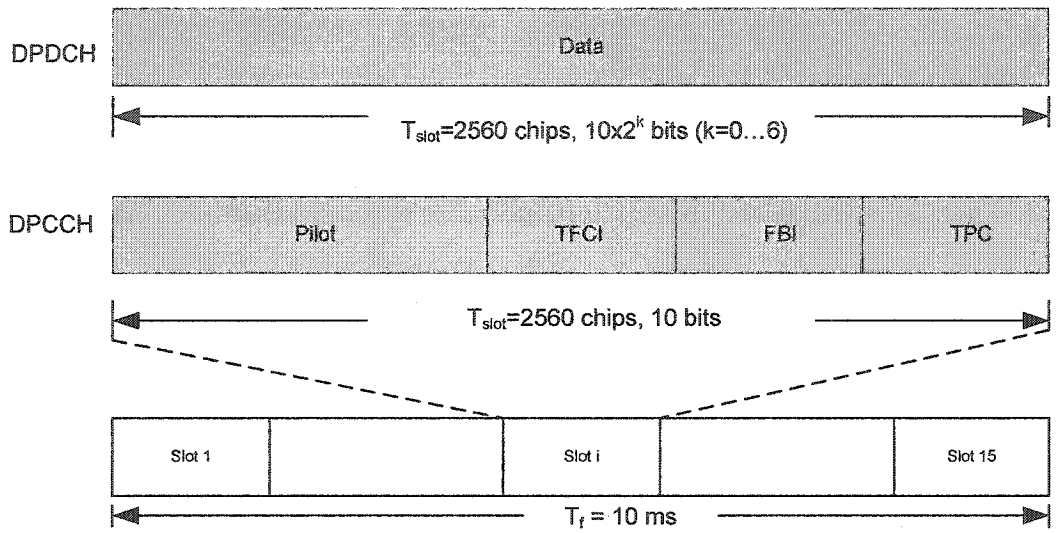

Figure 2-2: Uplink dedicated physical channel frame structure

Pilot bits can assist coherent demodulation and channel estimation. TFCI (transport format combination indicator) is used to indicate and identify several simultaneous services. Feedback Information (FBI) bits are used to support techniques requiring feedback. TPC (Transmit Power Control) is used for power control purpose. The exact number of bits of these different uplink DPCCH fields is given in [31]. The parameter k in Figure 2-2 determines the number of bits in each slot, and is related to spreading factor

of the physical channel by $SF = \frac{256}{2^k}$. The spreading factor thus may range from 256 down to 4. The spreading factor is selected according to the data rate.

2.3.2 Downlink Physical Channels

2.3.2.1 Downlink Dedicated Physical Channels

Figure 2-3 shows the frame structure of the downlink dedicated physical channels. As in the uplink, each frame of 10 ms is split into 15 slots; each slot is of the length of 2560 chips corresponding to one power control period.

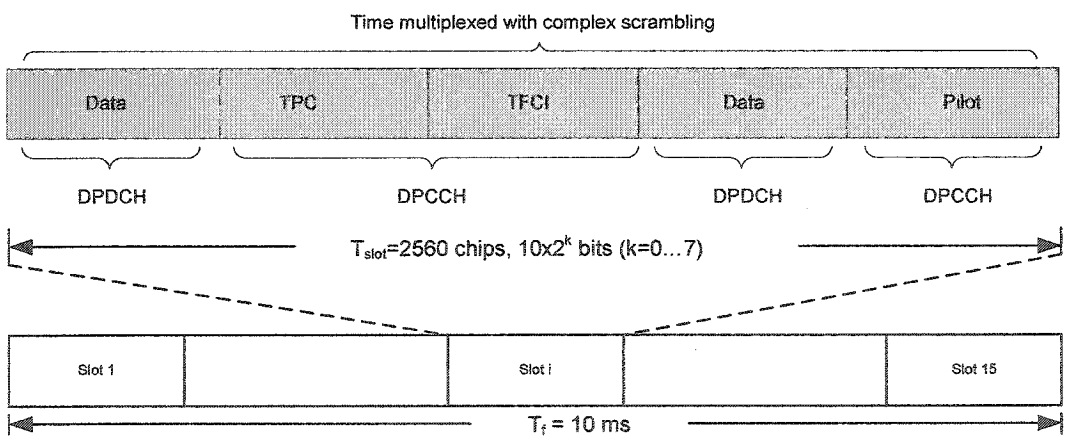

Figure 2-3: Downlink dedicated physical channel frame structure

The parameter k is related to the SF of the physical channel by $SF = \frac{512}{2^k}$. The spreading factor has a range of 4 to 512. Thus an additional spreading factor of 512 is permitted for the downlink. The different control bits have similar meanings to those in

the uplink. The exact number of bits in each downlink DPCH field is described in [31].

Pilot bits are used for coherent reception, power control signaling, and rate detection; they can also be used for adaptive antenna array training and equalization.

2.3.2.2 Downlink Common Pilot Channels (CPICH)

As in the uplink, the WCDMA downlink system transmits the pilot signal at the same time as the data signal. However, the pilot signal is both time-multiplexed into the data stream as shown in Figure 2-3, and transmitted continuously as the Common Pilot Channel (CPICH) as illustrated in Figure 2-4.

The CPICH channel uses a predefined bit/symbol sequence, transmitted at 15ksps (30kbps) with an SF of 256, as shown in Figure 2-4; it is used for downlink channel estimation as well as mobile terminal intra-frequency measurement of neighboring cells for soft handover.

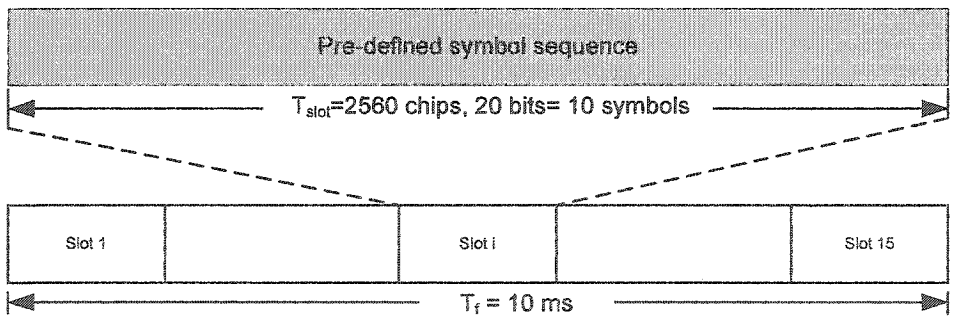

Figure 2-4: Frame structure of common pilot channel

2.4 Spreading and Modulation

In the spreading process, the physical channels are first spread to the channel bandwidth (3.84 Mcps) and then scrambled for cell or mobile terminal separation. First, we introduce the spreading code, and then we describe how the physical channels are spread and modulated in the uplink and downlink.

2.4.1 Spreading Code

The spreading code spreads the information data to the chip rate of 3.84 Mcps. The most important purpose of the spreading code is to help preserve orthogonality among different physical channels. In the WCDMA downlink, it is used for user identification; in the uplink, it is used for data/control channel separation. In WCDMA, Orthogonal Variable Spreading Factor (OVSF) codes are used as spreading codes. The OVSF codes can be picked from the code tree shown in the Figure 2-5 [4]. The subscript herein gives the spreading factor, and the argument within the parentheses provides the code number for that particular spreading factor.

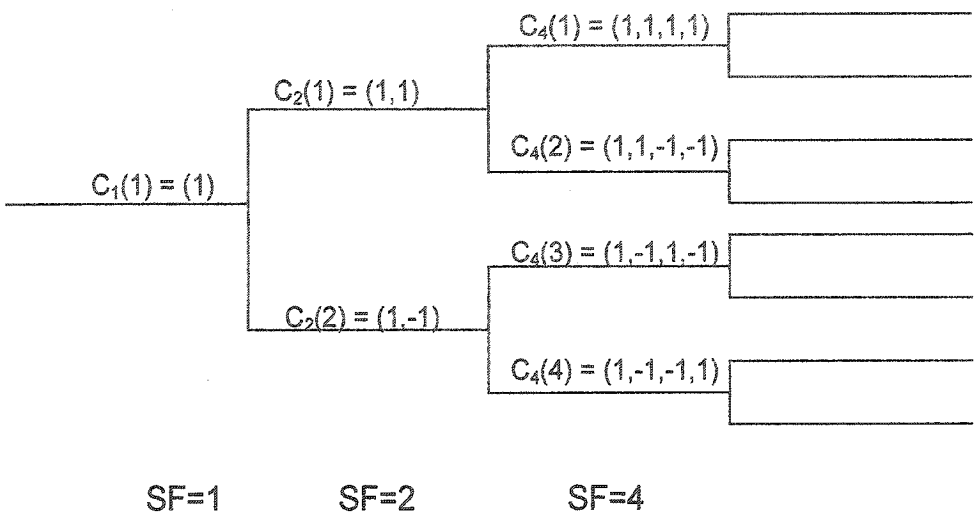

Figure 2-5: Code-tree for generation of OVSF codes

The spreading code length is in the form of 2^n, where n is greater than or equal to 2; it is also equal to the spreading factor ($SF = 2^n$). The use of OVSF codes allows the spreading factor to be changed and the orthogonality between different spreading codes of different lengths to be maintained. Any two codes of different levels are orthogonal to each other as long as one of them is not the root of the other code [8]. For example, the codes $c_{16}(2)$, $c_8(1)$ and $c_4(1)$ are all root codes of $c_{32}(3)$ and hence are not orthogonal to $c_{32}(32)$. A code can be used by a mobile terminal if and only if no other code on the path from the specific code to the root of the tree or in the sub-tree below the specific code is used by the same mobile terminal [33]. The generation method of OVSF can be explained with the help of the following matrix equations:

$$
\begin{bmatrix} c_1(1) \end{bmatrix} = 1
$$

$$
\begin{bmatrix} c_2(1) \\ c_2(2) \end{bmatrix} = \begin{bmatrix} c_1(1) & c_1(1) \\ c_1(1) & \overline{c_1(1)} \end{bmatrix} = \begin{bmatrix} 1 & 1 \\ 1 & -1 \end{bmatrix}
$$

$$
\begin{bmatrix} c_4(1) \\ c_4(2) \\ c_4(3) \\ c_4(4) \end{bmatrix} = \begin{bmatrix} c_2(1) & c_2(1) \\ c_2(1) & \overline{c_2(1)} \\ c_2(2) & c_2(2) \\ c_2(2) & \overline{c_2(2)} \end{bmatrix} = \begin{bmatrix} 1 & 1 & 1 & 1 \\ 1 & 1 & -1 & -1 \\ 1 & -1 & 1 & -1 \\ 1 & -1 & -1 & 1 \end{bmatrix}
$$

$$
\vdots
$$

$$
\begin{bmatrix} c_N(1) \\ c_N(2) \\ \cdot \\ \cdot \\ c_N(N-1) \\ c_N(N) \end{bmatrix} = \begin{bmatrix} c_{N/2}(1) & c_{N/2}(1) \\ c_{N/2}(1) & \overline{c_{N/2}(1)} \\ \cdot & \cdot \\ \cdot & \cdot \\ c_{N/2}(N/2) & c_{N/2}(N/2) \\ c_{N/2}(N/2) & \overline{c_{N/2}(N/2)} \end{bmatrix} \tag{2.21}
$$

In the above matrix notation, an over bar indicates binary complement (e.g. $\overline{1} = -1$ and $\overline{-1} = 1$) and N is an integral power of two. The first code of any code tree as described in this section is used to spread the DPCCH. This is a sequence of all 1's for any SF. The first DPDCH is spread by the code number (SF/4+1) where SF is the spreading factor for the data channel.

The spreading and modulation for the DPDCH and the DPCCH for both the links are described in the following two subsections.

2.4.2 Uplink Spreading and Modulation

As for the GSM system, discontinuous transmission in a WCDMA uplink can cause audible interference to audio equipment (such as a hearing aid) that is very close to the

terminal. Therefore, in a WCDMA uplink the two dedicated physical channels are I-Q code multiplexed instead of time multiplexed.

When data are present/absent (DTX), continuous transmission can be achieved with an I-Q code multiplexing control channel, as shown in Figure 2-6.

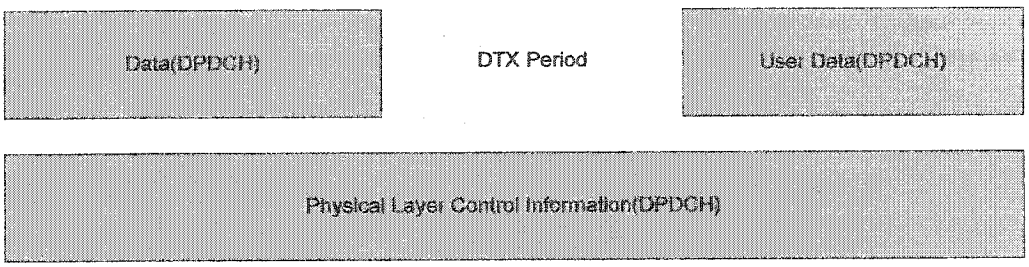

Figure 2-6: Parallel transmissions of DPDCH and DPCCH in the uplink

2.4.2.1 Uplink Spreading and Modulation

In the uplink, Binary Phase Shift Keying (BPSK) is used for data modulation of both the DPDCH and DPCCH. The modulated DPCCH is mapped to the Q-channel, while the first DPDCH is mapped to the I-channel. Subsequently added DPDCHs are mapped alternately to the I-channel or Q-channel. Spreading modulation is applied after data modulation and before pulse shaping. The spreading modulation used in the uplink is dual channel QPSK. Spreading modulation consists of two different operations. The first operation is spreading, where each data symbol is spread to the number of chips given by the spreading factor; this increases the bandwidth of the signal. The second operation is scrambling, where a complex valued scrambling code is applied to spread the signal.

Figure 2-7 shows the spreading and modulation for an uplink user haing a DPDCH and a DPCCH.

The bipolar data symbols on I and Q branches are independently multiplied by different channelization codes known as Orthogonal Variable Spreading Factor (OVSF) codes. OVSF codes are discussed in Section 2.4. The resultant signal is multiplied by a complex scrambling code which is a unique signature of the mobile station. The scrambled signal is then pulse shaped using the Square-Root Raised Cosine filter with a roll-off factor of 0.22. The pulse shaped signal is subsequently up-converted as shown in Figure 2-7. The application of a complex scrambling code with spreading modulation as described above is usually termed as Hybrid Phase Shift Keying (HPSK).

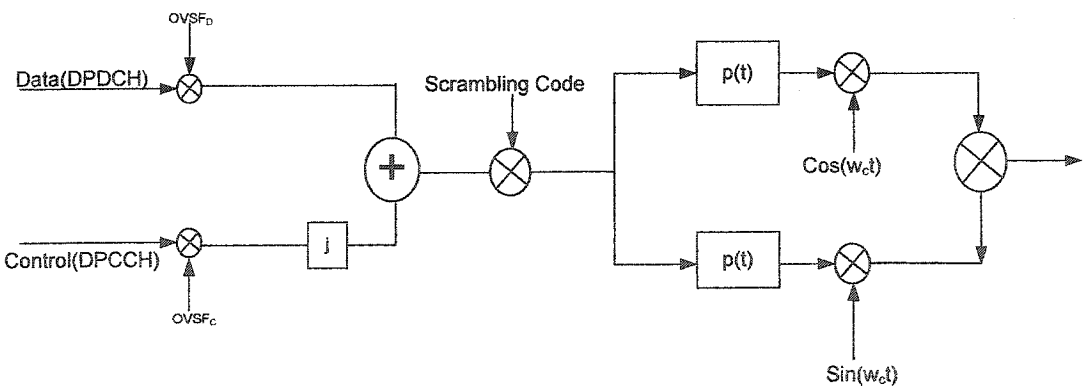

Figure 2-7: Uplink spreading and modulation

The spreading factor for the control channel is always set at the highest value, which is 256. This improves the noise immunity of the control channel by taking advantage of the highest possible processing gain.

2.4.3 Downlink Spreading and Modulation

The time-multiplexed solution is not used for the uplink since it would generate audible interference during discontinuous transmission. However, the audible interference generated with DTX is not a relevant issue for the downlink since the common channels have continuous transmissions.

A simple block diagram of a downlink transmitter for the 3GPP system is shown in Figure 2-8. Each bit of the Physical Channels (PCH) is Quadrature Phase Shift Keying (QPSK) modulated. Each pair of two bits is serial-to-parallel converted and mapped to the I and Q branches, respectively. The modulated I (in-phase) and Q (quadrature) bits are channelized by multiplying Orthogonal Variable Spreading Factor (OVSF) codes at the chipping rate of 3.84 Mcps. All channelized signals are combined first and then scrambled by a long code, which is generated from the Gold code set. The scrambled signal and the unscrambled signal of the Synchronization Channel (SCH) are combined together. The combined signal is pulse-shaped by a root-raised cosine FIR filter with a roll-off factor of α = 0.22. A detailed description of the 3GPP WCDMA system is available in [4] and [31]-[34].

Figure 2-8 shows the spreading and modulation for a downlink user. The downlink user has a DPDCH and a DPCCH. Additional DPDCHs are QPSK modulated and spread with different channelization codes. The OVSF codes have been described in Section 2.4.1.

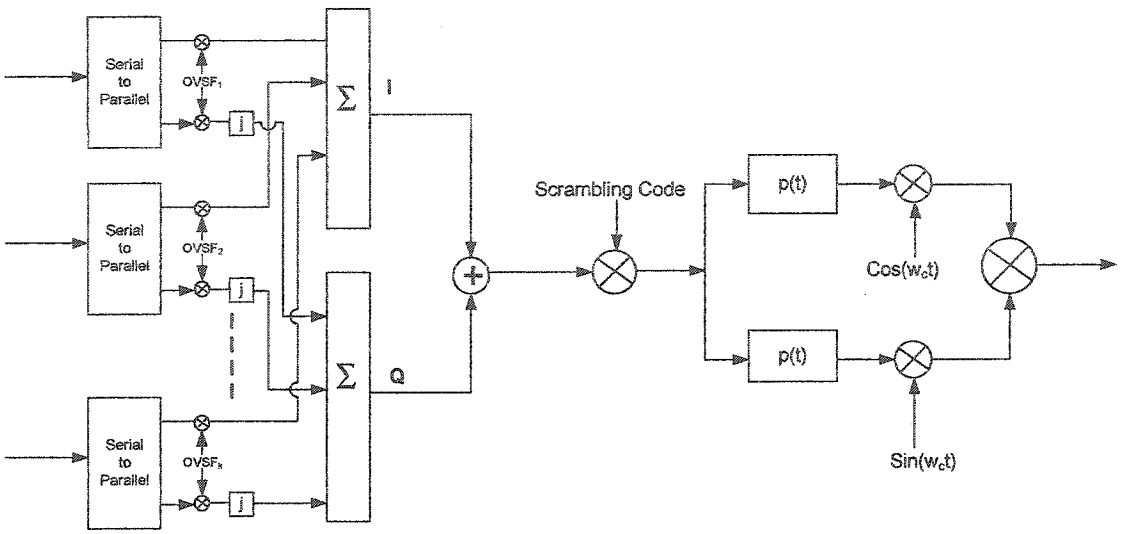

Figure 2-8: Block diagram of a downlink transmitter for the 3GPP WCDMA system

We can observe some differences between the spreading and modulation in the downlink and that in the uplink. The data modulation is QPSK in the downlink whereas it is BPSK in the uplink. The data rates in the I and Q channels are the same in the downlink whereas they may be different in the uplink. The scrambling code is cell specific in the downlink, whereas it is mobile station specific in the uplink. As in the uplink, square-root raised cosine filters with a roll-off factor of 0.22 are employed for pulse shaping in the downlink.

2.5 Multipath Fading Channel and Rake Receiver

Reception of a direct-sequence spread signal allows the use of a more efficient reception technique. One of the key problems in wireless communications is the

distortion of the transmitted signal introduced by the radio channel. But repeatedly transmitted information at a time spacing that exceeds the coherence time of the channel can provide time diversity. The inherent time diversity of the mobile radio channel can be exploited when using SS technology. For frequency selective fading, the signal bandwidth is much greater than the coherence bandwidth of the channel; therefore, multipath components are resolvable and independent of each other [4], [17]. The RAKE receiver, which was proposed in 1958 first by Price and Green, is essentially a diversity receiver designed specifically for CDMA, where the diversity is provided by the fact that the multipath components are practically uncorrelated with one another when their relative propagation delays exceed a chip period.

RAKE receivers take advantage of the energy present in multipath components by correlating with each path. The RAKE receiver is composed of several fingers which each resemble a single correlator and have a different time delay and phase rotation matched to one multipath component. The resolution of the RAKE (i.e. the ability to resolve between separate multipaths) is dependent on the chip rate of the system. Figure 2-9 shows a general RAKE receiver [17]. There are several methods for choosing the weights to combine the fingers.

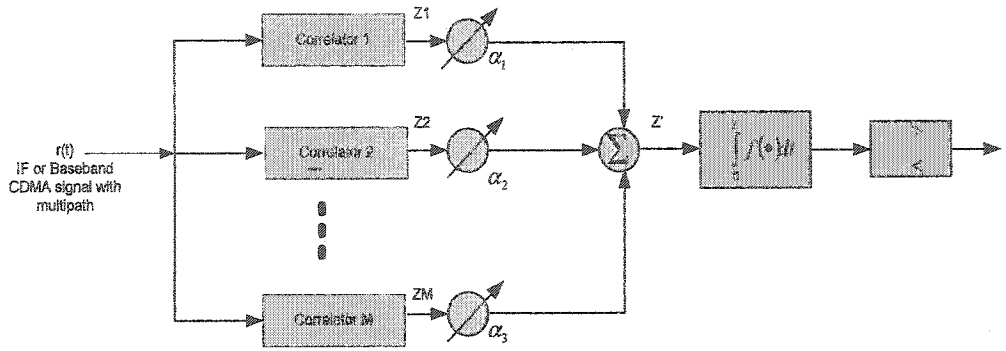

Figure 2-9: RAKE receiver with M fingers

A RAKE receiver consists of a bank of correlators, each of which is used to detect separately one of the M strongest multipath components. The outputs of each correlator are weighted to provide a better estimate of the transmitted signal than that provided by a single component. Demodulation and bit decision are then based on the outputs of the M correlators. If just one correlator is used in the receiver, the output value cannot be corrected once the output of the correlator has been corrupted by fading. However, in a RAKE receiver, if the output from one correlator is corrupted by fading, the others may not be, and the corrupted signal may be discounted through the weighting process. The conventional RAKE receiver improves the system performance through temporal diversity, by using a combination of delayed replicas of the desired signal.

It is well known that the traditional RAKE receiver separately tracks and coherently recombines the multipath components of the received signal. In particular, the RAKE structure consists of a tapped delay line with variable delays, whereby each delayed version of the received signal is correlated with the spreading waveform of the desired user. The outputs of the correlators are then conveniently combined to maximize the SNR

at the receiver output [17].

2.6 Summary

In this chapter, the fundamentals of WCDMA systems have been presented. The concept of spread spectrum and the Code Division Multiple Access (CDMA) technique have first been reviewed. A physical layer description of the radio access network of a WCDMA FDD system is then provided. The spreading and modulation operation for physical channels in both uplink and downlink has been discussed in detail. We have also presented multipath channels and the Rake receiver technique, which is one of the performance enhancing schemes used in DS-CDMA systems.

As shown in this chapter, we can use the dedicated pilot bits in both uplink and downlink for employing adaptive antennas, namely, smart antennas, at the receiver in order to increase the capacity and coverage of the system. This notable performance-enhancing scheme will be detailed in the following chapters.

Chapter 3

Smart Antenna Techniques

3.1 Introduction

Smart antenna technology can be defined as the art of combining the signals from/to an array of small-gain antennas, which is used to suppress the noise and interference [9], [13], [14]. Usually, a wireless channel has non-ideal behavior. In many cases, there is an obstruction of the direct ray, so the receiving antenna sees only reflected rays. This is the so-called Rayleigh channel. The envelope and phase of the received signal in Rayleigh channel vary when the transmitter or receiver are moving. The damaging effects of fading may be particularly important in the case of deep fading, where the signal amplitude decreases dramatically. An array of antennas uses spatial diversity to minimize the effect of deep fading, exploiting the fact that when a signal from one direction (or from one antenna) is suffering from a dip, the signals from other directions (or antennas) may be not. Furthermore, a smart antenna array with a fixed number of antenna elements and space-time processing could offer a broad range of ways to improve wireless system performance. It could provide enhanced coverage through range extension, hole filling and better building penetration, and might also be used to increase long-term system

capacity [15]. By changing the phase and amplitude of the exciting currents in each of the antenna elements, an adaptive antenna is able to change its antenna pattern dynamically according to noise, interference and multipaths, and it can adjust its pattern to scan the main beam and/or place nulls in any direction. Adaptive antennas are used to form beams for transmission and may also be used to enhance received signals. Smart antenna systems can include both switched beam technologies and adaptive antenna arrays. Switched beam systems generate a number of fixed beams at an antenna site. The receiver selects the beam that provides the greatest signal enhancement and interference reduction. Switched beam systems may not offer the degree of performance improvement as offered by adaptive systems, but they are often much less complex and are easier to retrofit to existing wireless technologies.

This chapter reviews basic concepts related to antenna arrays and discusses adaptive beamforming techniques. Section 3.2 introduces antenna array concepts and the array response model. Section 3.3 presents antenna array beamforming and spatial filtering methods. Different algorithms for adaptive antennas and spatial filtering are presented in Section 3.4. This chapter also investigates the effects of different parameters that influence the beamforming ability. The simulation results are presented for both noise-free and noisy channels.

3.2 Antenna Array and Response Model

An antenna array uses a fixed set of antennas of low-gain antenna elements which are connected by a combining network. The antenna elements in an antenna array can be arranged in various geometries (e.g., linear, circular, planar) with reference to a common fixed point. The radiation pattern of an array is determined by the radiation pattern of the individual elements, their orientation and relative positions in space, as well as the amplitude and phase of the currents feeding the array elements. In the case of a linear array, the centers of the elements of the array are aligned along a straight line, as shown in Figure 3-1. If the spacing between the elements is equal, it is called a Linear Equally Spaced array (*LES*).

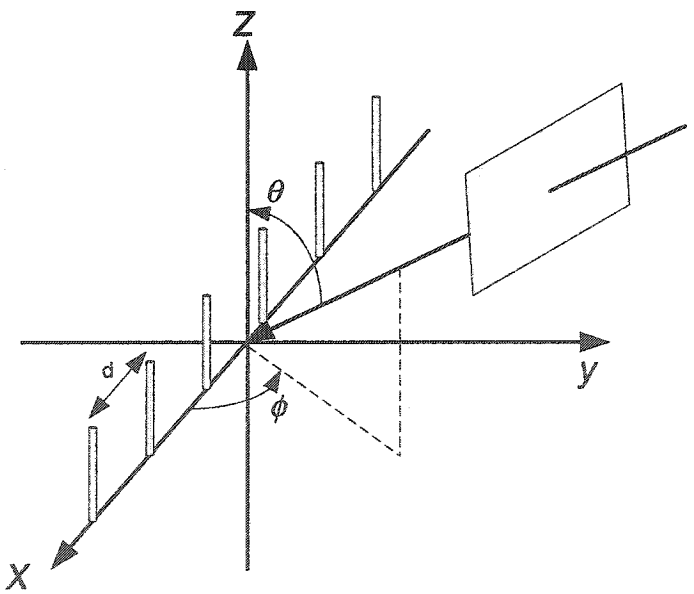

Figure 3-1: A linear spaced array oriented along the X-axis, receiving a plane wave from direction (θ, φ)

We mainly discuss the performance of the commonly used LES antenna array model.

To simplify the analysis, we make the following assumptions [15]:

---The spacing between array elements is small enough such that there is no amplitude variation between the signals received at different elements.

-----There is no mutual coupling between elements.

--- All incident fields can be decomposed into a discrete number of plane waves. This means there are a finite number of signals.

3.2.1 Linear Equally Spaced Array

As shown in Figure 3-2, we assume that the antenna array includes M elements, each being equally spaced by a distance d, and a plane wave arrives at the array from a direction (θ, φ) off the array broadside. The angle (θ, φ) is called the direction-of-arrival (DOA) of the received signal, and is measured clockwise from the broadside of the array. Consider the case in which a wave is incident on the array shown in Figure 3-2 in the x, y (horizontal) plane so that $\theta = \pi/2$. This is a reasonable approximation for many cellular and PCS smart antenna applications.

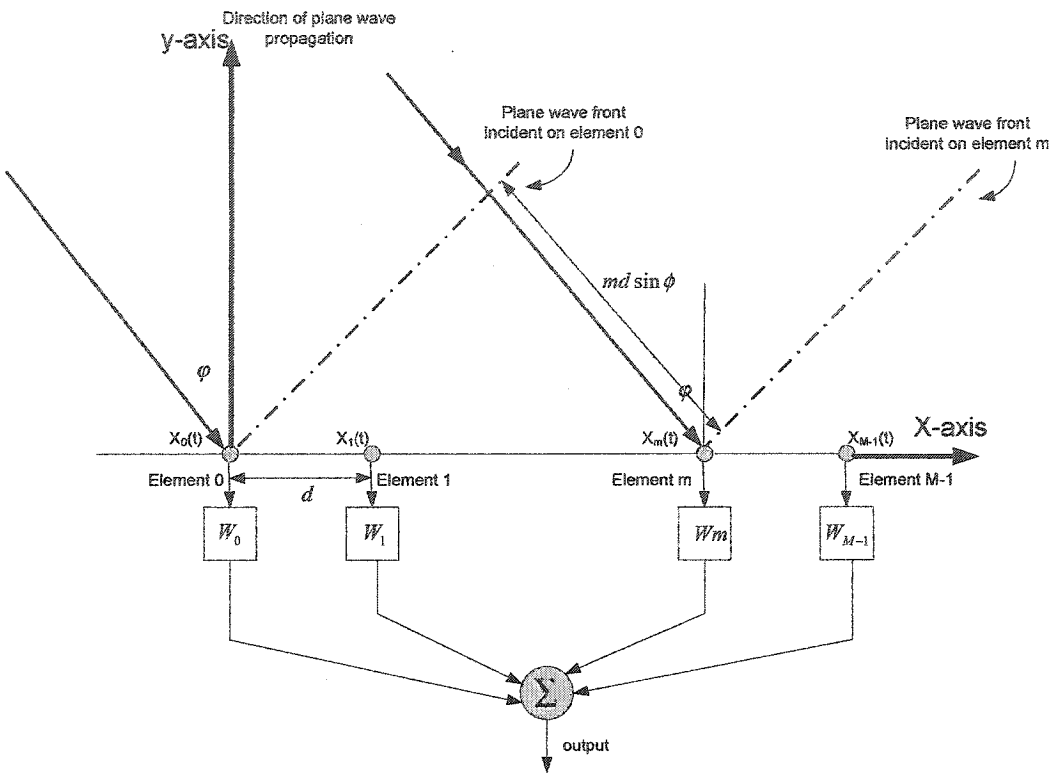

Figure 3-2: Illustration of plane wave incident from direction (θ, φ) on an M-element LES antenna array with inter-element spacing of d

We use the complex envelope representation $x_0(t)$ to express the received signal at the first element. Now taking the first element in the array as the reference point, if the signals have originated far away from the array, and this plane wave advances through a non-dispersive medium that only introduces propagation delays, the output of any other array elements can be represented by a time-advanced or time-delayed version of the signal at the first element. From Figure 3-2, we see that the plane wave-front at the first element should propagate through a distance $d\sin\varphi$ to arrive at the second element. The time delay due to this additional propagation distance is given by

$$\tau = d\sin\varphi / c \tag{3.1}$$

where c is the light velocity, $3\times10^8 m/s$. The effect of the time delay on the signal can be represented by a phase shift term $\exp\{-j(2\pi f_c\tau)\}$. So, we have the complex envelope of the received signal in element 1,

$$x_1(t) = x_0(t)\exp\left\{-j(2\pi f_c\frac{d\sin\varphi}{c})\right\}$$

$$= x_0(t)\exp\left\{-j(\frac{2\pi}{\lambda}d\sin\varphi)\right\} \tag{3.2}$$

where $\beta = 2\pi/\lambda$ is the phase propagation factor, λ denotes the free space wavelength of the carrier, given by c/f_c, and f_c is the carrier frequency in Hz.

Similarly, for element m, the complex envelope of the received signal can be expressed as

$$x_m(t) = x_0(t)\exp\left\{-j(\frac{2\pi}{\lambda}md\sin\varphi)\right\} \qquad m = 0,...,M-1 \tag{3.3}$$

Letting

$$\mathbf{x}(t) = \begin{bmatrix} x_0(t) \\ x_1(t) \\ . \\ . \\ x_{M-1}(t) \end{bmatrix} \tag{3.4}$$

$$\mathbf{f}(\varphi) = \begin{bmatrix} 1 \\ e^{-j(\frac{2\pi}{\lambda}d\sin\varphi)} \\ . \\ . \\ e^{-j(\frac{2\pi}{\lambda}(M-1)d\sin\varphi)} \end{bmatrix}, \tag{3.5}$$

the signal input to an antenna array with M elements may be expressed in vector form as

$$\mathbf{x}(t) = \mathbf{f}(\varphi)x_0(t) \tag{3.6}$$

where $\mathbf{x}(t)$ is the array input data vector, and $\mathbf{f}(\varphi)$ is often called the steering vector. In general, the steering vector is a function of the individual element response, array geometry and signal frequency. However, in this case the steering vector is only a function of the angle-of-arrival.

In wireless communications, there are usually more signals impinging on the array. These may be caused by multipath propagation or may come from other interference sources, such as neighboring base stations or mobile terminals. These signals may be uncorrelated, or can be partially correlated due to the noise corruption, as happened in multipath propagation, where each path is a scaled and time-delayed version of the original transmitted signal. Suppose that there are signals $s_1(t),....,s_Q(t), Q = N \times L$, which are centered around the same carrier frequency, say f_c, with a DOA of φ_i, $i = 1,2,....,Q$. For downlink, N is the number of neighboring base stations (BS) to the mobile terminal and L is the number of multipath components between each BS and the mobile terminal; for uplink, N is the number of user signals transmitted from different locations, and L denotes the number of multipath components that arrive at the array for each user signal. We further assume that all of the multipath components for a particular user arrive within a time window which is much less than the channel symbol period for that user.

The received signal at the array is a superposition of all the impinging signals and noise. Therefore, the input data vector may be expressed as

$$\mathbf{x}(t) = \sum_{q=1}^{Q} a_q \mathbf{f}(\varphi_q) s_q(t) + \mathbf{n}(t) \tag{3.7}$$

where a_q is the complex amplitude of the l^{th} multipath component for the n^{th} user/ base station, φ_q is the DOA of the l^{th} multipath component for the n^{th} user / base station, $\mathbf{f}(\varphi_q)$ is the steering vector corresponding to φ_q, and

$$\mathbf{f}(\varphi_q) = \begin{bmatrix} 1 \\ e^{-j(\frac{2\pi}{\lambda} d \sin\varphi_q)} \\ . \\ . \\ e^{-j(\frac{2\pi}{\lambda}(M-1) d \sin\varphi_q)} \end{bmatrix} \tag{3.8}$$

and $\mathbf{n}(t)$ denotes the $M \times 1$ vector of the noise at the array elements. In matrix notation, the most commonly used input data model can be represented as

$$\mathbf{x}(t) = \mathbf{F}(\Phi)\mathbf{s}(t) + \mathbf{n}(t) \tag{3.9}$$

where $\mathbf{F}(\Phi)$ is the $M \times Q$ matrix of the steering vectors

$$\mathbf{F}(\Phi) = \left[\mathbf{f}(\varphi_1) \quad \mathbf{f}(\varphi_2) \quad \ldots \quad \mathbf{f}(\varphi_Q)\right] \tag{3.10}$$

and

$$\mathbf{s}(t) = \begin{bmatrix} s_1(t) \\ s_2(t) \\ . \\ . \\ s_Q(t) \end{bmatrix} \tag{3.11}$$

After receiving the signals arriving at the antenna array, if we know the Direction of Arrival (DOA) of every signal, we could use a type of processing called beamforming to form beams that simultaneously receive a signal radiating from a specific location and attenuate signals from other locations. In what follows, we will focus on beamforming

and spatial filtering.

3.3 Spatial Filtering and Beamforming Array Response

3.3.1 Spatial Filtering

Systems designed to receive spatially propagating signals often encounter the interfering signals. Adaptive antennas exploit the inherent spatial diversity of the mobile radio channel, provide an antenna gain and enable spatial interference suppression. Thus, they meet the high spectral efficiency and quality requirements of the third generation mobile radio systems.

Fortunately, the desired and interfering signals usually originate from different spatial locations. This spatial separation can be exploited to separate signal from interference using a spatial filter at the receiver. A beamformer is a processor used in conjunction with an array of sensors (i.e., antenna elements in an adaptive array) to provide a versatile form of spatial filtering. The sensor array collects spatial samples of propagating wave fields, which are processed by the beamformer. Typically, a beamformer linearly combines the spatially sampled time series from each sensor to obtain a scalar output time series. In the same manner, an FIR filter linearly combines temporally sampled data.

The baseband complex envelope representation of the M-element antenna array is shown in Figure 3-2. Each branch of the array has a weighting element, w_m. The weight

w_m has both a magnitude and a phase associated with it. Assume that all of the array elements are noiseless isotropic antennas that have uniform gain in all directions. Let us consider the case of having only one desired user represented by the baseband complex envelope $s(t)$. Then, the signal received at antenna element m is given by

$$u_m(t) = As(t)e^{-j\omega_c\tau_m} \tag{3.12}$$

where A is the arbitrary gain, w_c is the carrier frequency and τ_m represents the time delays of the wave on the m^{th} element relative to a reference point. The signal Z(t) at the array output is:

$$Z(t) = \sum_{m=0}^{M-1} w_m^{*} u_m(t) = As(t)\sum_{m=0}^{M-1} w_m^{*} e^{-j\omega_c\tau_m} = As(t)G(F) \tag{3.13}$$

where * denotes the complex conjugate. Since we are now using the complex envelope representation of the received signal, both $u_m(t)$ and w_m are complex. In the following discussion, each sensor is assumed to have all necessary receiver electronics and A/D converters, and the beamforming is performed digitally. Here we set the complex weight $w_m = a_m e^{j\omega_c\hat{\tau}_m}$ with fading a_m and the time delay $\hat{\tau}_m$, which are applied to the output of the m^{th} antenna element.

The array response of a weighted antenna array, which represents the relative sensitivity of a response to signals coming from DOA φ and having an array response vector of $\mathbf{g}(\varphi)$, can be defined as

$$G(\Phi) = \mathbf{W}\mathbf{g}(\varphi) = \sum_{m=0}^{M-1} w_m e^{-j\omega_c\tau_m} = \sum_{m=0}^{M-1} a_m e^{-j\omega_c(\tau_m - \hat{\tau}_m)} \tag{3.14}$$

The array factor determines the ratio of the received signal available at the array output,

z(t), to the signal As(t). By adjusting the weight, w_m, it is possible to set the maximum of the main beam of the array factor to any desired direction.

Noting that $\hat{\tau}_m$ is a value related to the desired DOA φ_0 and recalling (3.1), we set w_m with

$$\hat{\tau}_m = m \cdot \frac{d}{c} \cos\varphi_0 \tag{3.15}$$

So, (3.14) can be rewritten as:

$$G(\Phi) = \sum_{m=0}^{M-1} a_m e^{-j\omega_c(\tau_m - \hat{\tau}_m)} = \sum_{m=0}^{M-1} a_m e^{-j(2\pi m)\frac{d}{c}(\cos\varphi - \cos\varphi_0)} \tag{3.16}$$

In a special case where $a_m = 1$ for m = 0, 2, ...M-1, using the equality $\sum_{m=0}^{M-1} x^m = \frac{1-x^M}{1-x}$, (3.16) can be rewritten as

$$G(\Phi) = \sum_{m=0}^{M-1} e^{-j\omega_c(\tau_m - \hat{\tau}_m)} = \frac{1 - e^{-j\frac{2\pi}{\lambda}Md(\cos\varphi - \cos\varphi_0)}}{1 - e^{-j\frac{2\pi}{\lambda}d(\cos\varphi - \cos\varphi_0)}} \tag{3.17}$$

$$= \frac{\sin(\frac{2\pi}{\lambda}Md(\cos\varphi - \cos\varphi_0))}{\sin(\frac{2\pi}{\lambda}d(\cos\varphi - \cos\varphi_0))} e^{-j\frac{2\pi}{\lambda}Md(\cos\varphi - \cos\varphi_0)} \tag{3.18}$$

The beam pattern is defined as the magnitude of the array response $|G(\Phi)|$.

3.3.2 Beamforming Results

Simulation results for the proposed multi-target space-time receiver (MT-STR) are obtained using Matlab. Initially we assume a stationary user terminal with an infinite

signal-to-noise ratio, or a noise free channel model. First we will show how an antenna array improves the performance of a conventional receiver. For a WCDMA downlink system with f_c=2.14GHz and $\lambda = 14cm$, we analyze the effect on the beam pattern (i.e., the spatial filtering ability) caused by different choices for the antenna array spacing d and the number of antenna array elements used. Later we will show how the receiver performs with an adaptive antenna array in a noisy environment.

Figure 3-3 shows the beam steering ability of an MT-STR receiver using a LES antenna array with 4 antenna elements and a spacing of 0.25λ, and spatial adapters with steering angles φ_0 of 0^0, 75^0, 120^0 and 270^0, respectively. We can see from the figure that each spatial adapter can form a beam pattern towards the desired user.

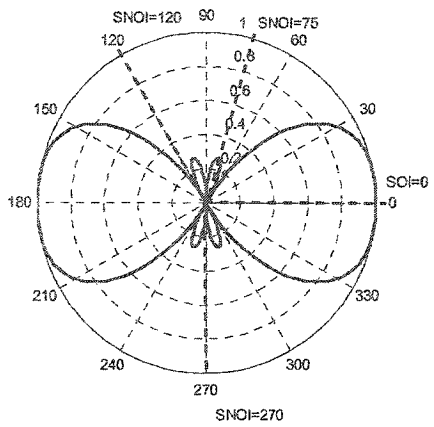

(a) Steering at 0^0

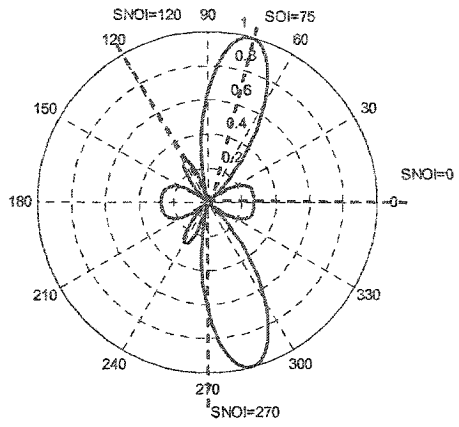

(b) Steering at 75^0

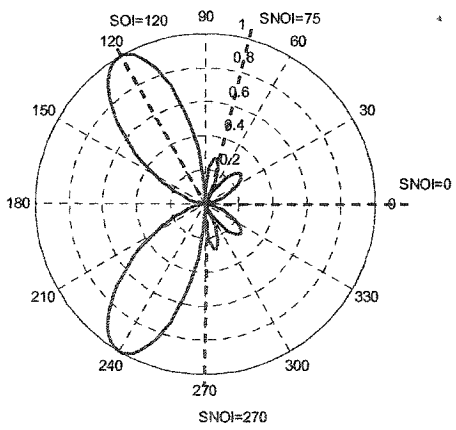

(c) Steering at 120^0

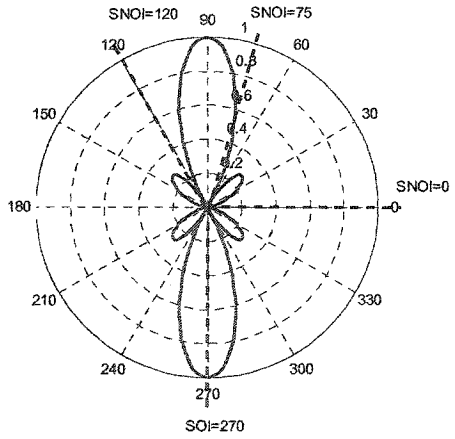

(d) Steering at 270^0

Figure 3-3: Beam patterns of 4-element LES antenna array with $d = 0.25\lambda$

We now investigate the effect on the beam pattern of both the spacing d between antenna elements and the number of antenna elements.

Figures 3-4, 3-5 and 3-6 show the beam steering ability of an LES antenna array with

4 elements, three distances 0.125λ, 0.25λ and 0.5λ, and two steering angles φ_0 of 0^0 and 60^0.

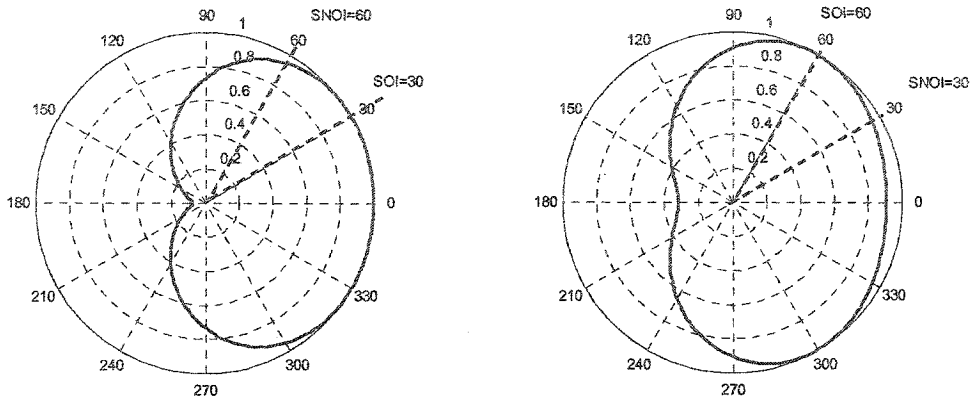

a) Steering at 30^0 (b) Steering at 60^0

Figure 3-4: Beam patterns of 4-element LES antenna array with d= 0.125λ

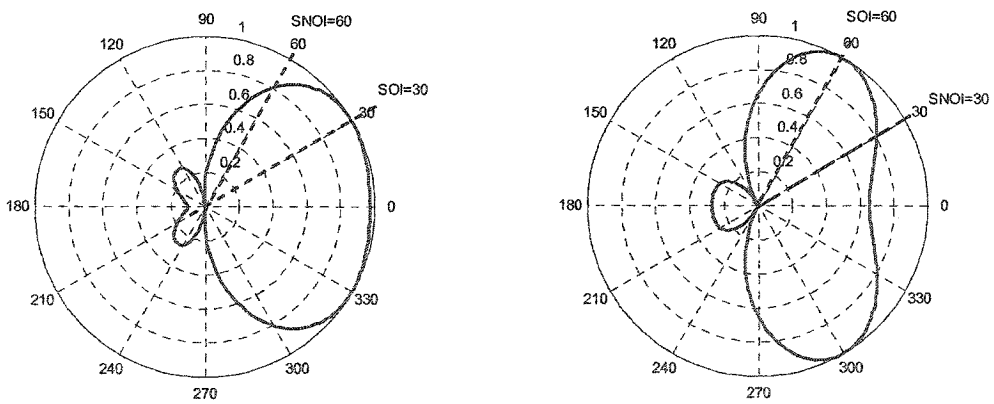

(a) Steering at 30^0 (b) Steering at 60^0

Figure 3-5: Beam patterns of 4-element LES antenna array with d= 0.25λ

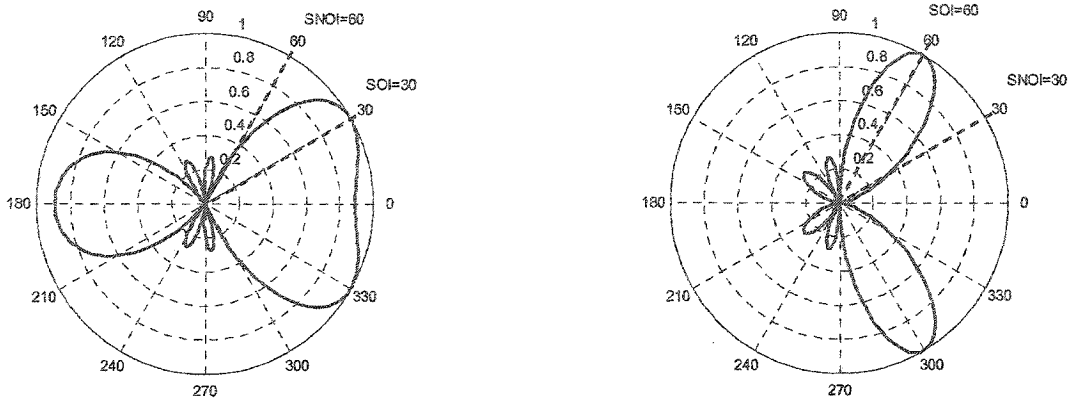

(a) Steering at 30^0 (b) Steering at 60^0

Figure 3-6: Beam patterns of 4-element LES antenna array with d= 0.5λ

From these simulation results, we can see that distances of 0.25λ and 0.125λ can provide good beamforming ability. In WCDMA systems with $f_c = 2.14GHz$, 0.25λ is translated to 3.5cm, which is suitable for use in mobile terminals. Figure 3-7 shows the beam patterns of a 2-element LES antenna array with a distance of d= 0.25λ.

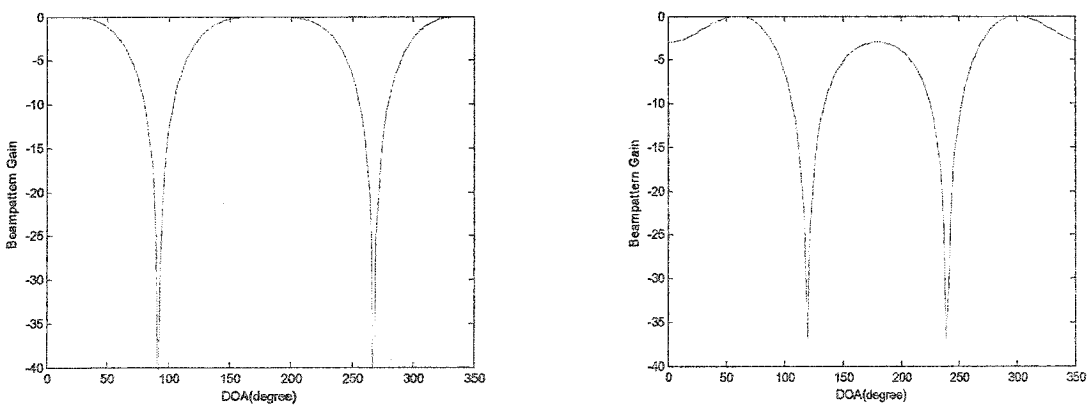

(a) Steering at 0^0 (b) Steering at 60^0

Figure 3-7 : Beam patterns of 2-element LES antenna array with d= 0.25λ

Figures 3-8, 3-9, 3-10 show the beam steering ability of two LES antenna arrays with

3, 5 and 8 elements, respectively, where the steering angle φ_0 is set to 0^0 and 60^0, the spacing of two adjacent elements is d=0.5λ. Comparing the beam pattern of 4 elements with d=0.5λ in Figure 3-6, it can be seen that more antenna elements provide better beamforming ability.

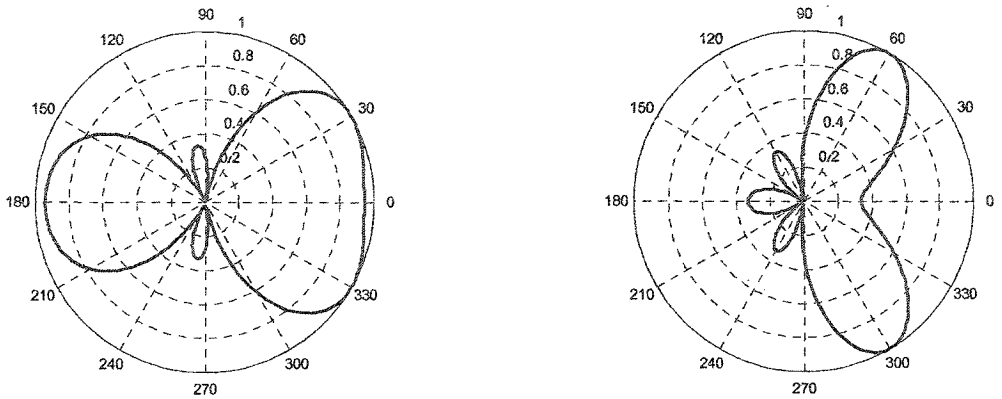

(a) Steering at 30^0 (b) Steering at 60^0

Figure 3-8: Beam patterns of 3-element LES antenna array with d=0.5λ

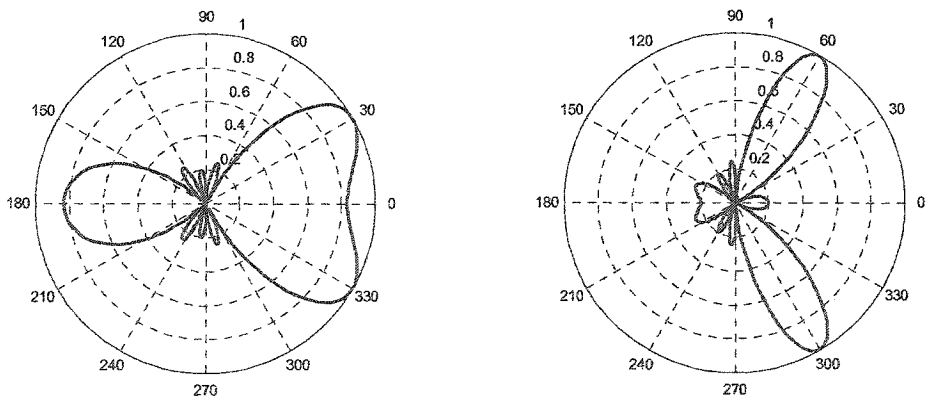

(a) Steering at 30^0 (b) Steering at 60^0

Figure 3-9: Beam patterns of 5-element LES antenna array with d=0.5λ

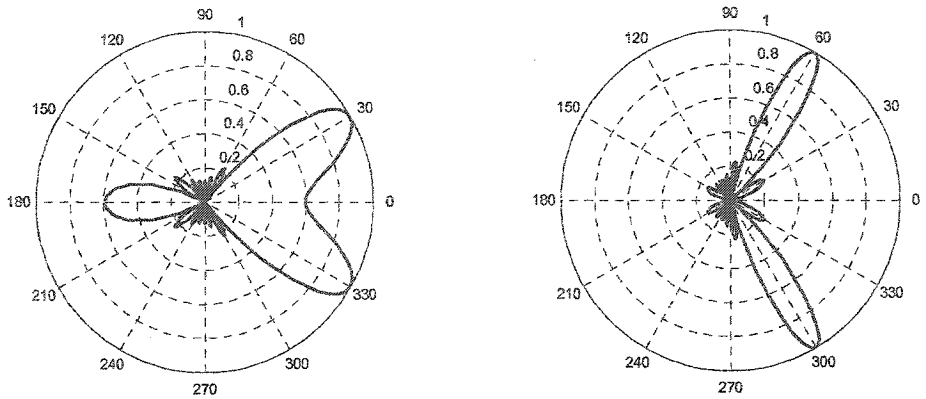

(a) Steering at 30^0 (b) Steering at 60^0

Figure 3-10: Beam patterns of 8-elements LES antenna array with d=0.5λ

3.4 Adaptive Arrays

The DOAs of the received signals at the antenna array are time varying due to the movement of mobile devices. To track these time-varying factors, an adaptive array can be used. An adaptive array is an antenna system that can modify its beam pattern or other parameters automatically in response to the signal environment. Also, since the data used for estimating the optimal solution are noisy, it is desirable to reduce the effects of the noise by using an update technique. An adaptive algorithm is used to periodically update the weight vector. A simple adaptive array is shown in Figure 3-11. By means of internal feedback control while the antenna system is operating, an adaptive array processor can extract signal k using a weight vector $\mathbf{w}$. The weight vector must be updated or adapted periodically.

In adaptive antenna techniques, a weight vector is determined which minimizes a

cost function. Typically, this cost function represents a performance criterion, such as minimum Mean Squared Error (MSE), maximum Signal-to-Interference-and-Noise Ratio (SINR), minimum noise variance etc; the cost function is inversely associated with the quality of the signal at the array output. As the weights are iteratively adjusted, the cost function becomes smaller and smaller. When the cost function is minimized, the performance criterion is met and the algorithm is said to be convergent [44].

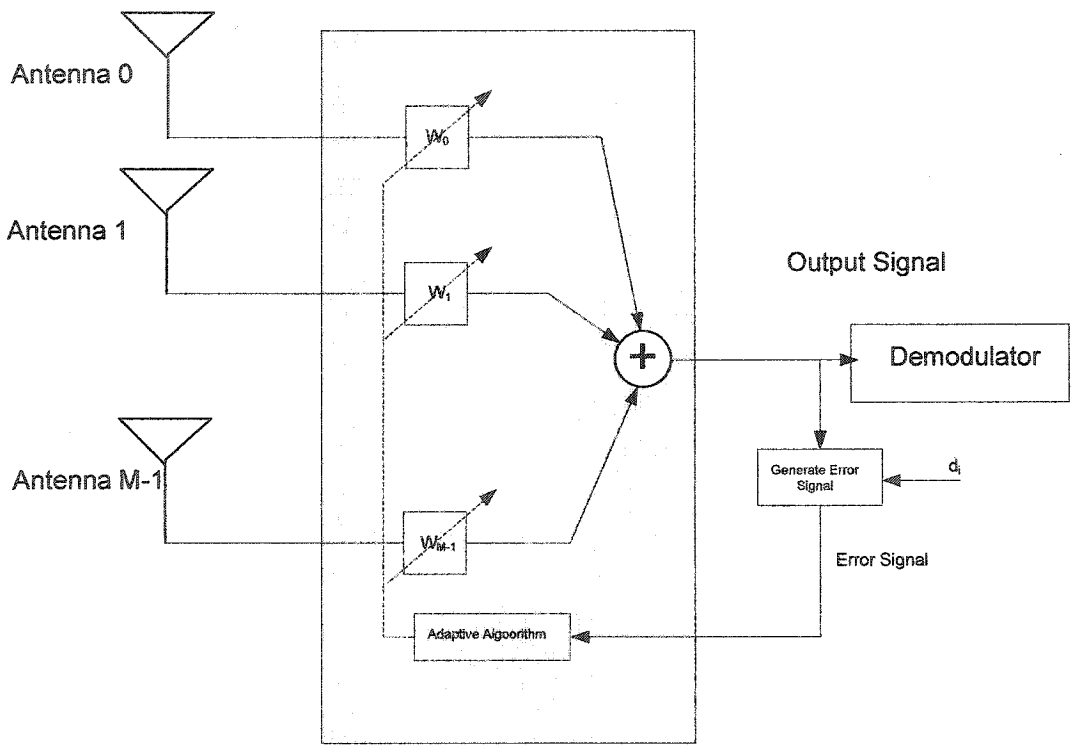

Figure 3-11: An adaptive antenna structure

There are a variety of existing adaptive algorithms to adjust the weight vector. The choice of one algorithm over another is determined by various factors [39] such as the rate of convergence (defined as the number of iterations required for the algorithm, in response to stationary input, to converge to the optimum solution), tracking ability to the

variations in the environment and computational complexity. Two of the most popular techniques that have been applied extensively in communication systems are the Minimum Mean Square Error (MMSE) and the Least Square (LS) criteria.

3.4.1 Minimum Mean Square Error (MMSE) Solution

MMSE solutions are posed in terms of ensemble averages and produce a single weight vector, w_k, which is optimal over the ensemble of possible realizations of the stationary environment. This is the approach used in classical Wiener filter theory.

In the MMSE approach, for an input signal $x(t)$, the cost function to be minimized is the mean-squared error between the desired signal $d(t)$ and the array output $y(t)$ [44]. Let $x(k)$, $y(k)$ and $d(k)$ denote the sampled signal of $x(t)$, $y(t)$ and $d(t)$ respectively at time t_k. Then,

$$y(k) = \mathbf{w}^H \mathbf{x}(k) \tag{3.19}$$

The error signal is given by

$$e(k) = d(k) - y(k) \tag{3.20}$$

and the mean-squared error is defined by

$$J = E\left[\left|e(k)^2\right|\right] \tag{3.21}$$

where $E[\ ]$ denotes the ensemble expectation operator. Substituting (3.19) and (3.20) into (3.21), we obtain the cost function as given below

$$J = E\left[\left|d(k) - y(k)\right|^2\right]$$

$$= E\left[\{d(k) - y(k)\}\{d(k) - y(k)\}^*\right]$$

$$= E\left[\{d(k) - \mathbf{w}^H \mathbf{x}(k)\}\{d(k) - \mathbf{w}^H \mathbf{x}(k)\}^*\right]$$

$$= E\left[|d(k)|^2 - d(k)\mathbf{x}^H(k)\mathbf{w} - \mathbf{w}^H \mathbf{x}(k)d^*(k) + \mathbf{w}^H \mathbf{x}(k)\mathbf{x}^H(k)\mathbf{w}\right] \qquad (3.22)$$

Note that the cost function is a second order function of the weight vector and has a unique minimum value. These features imply that (3.22) will always converge monotonically to a unique minimum value corresponding to the weight vector w_{opt} [15].

In general, we can minimize a vector function by determining a location where the gradient of the function gets zero. As the weight is a complex vector $w_i = a_i + jb_i$, using the definition of the gradient of a function of a complex vector, we obtain [15]

$$\nabla(\mathbf{w}^H \mathbf{A}\mathbf{w}) = 2\mathbf{A}\mathbf{w}$$

$$\nabla(\mathbf{w}^H \mathbf{C}) = 2\mathbf{C}$$

$$\nabla(\mathbf{C}^H \mathbf{w}) = 0$$

Therefore, we have

$$\nabla J(w_k) = 2E\left[\mathbf{x}(k)\mathbf{x}^H(k)\right]\mathbf{w}_k - 2E\left[\mathbf{x}(k)d^*(k)\right] = 2\mathbf{R}\mathbf{w}_k - 2\mathbf{P} \qquad (3.23)$$

where $\mathbf{R}$ is the $M \times M$ correlation matrix of the input data vector $\mathbf{x}(k)$, i.e.,

$$\mathbf{R} = E\left[\mathbf{x}(k)\mathbf{x}^H(k)\right] \qquad (3.24)$$

And $\mathbf{P}$ is the $M \times 1$ cross-correlation vector between the input data vector and the desired signal $d(k)$, i.e.,

$$\mathbf{P} = E\left[\mathbf{x}(k)d^*(k)\right] \qquad (3.25)$$

setting the gradient of the cost function equal to zero, we have

$$-2\mathbf{P} + 2\mathbf{R}\mathbf{w}_{opt} = 0 \tag{3.26}$$

or equivalently

$$\mathbf{R}\mathbf{w}_{opt} = \mathbf{P} \tag{3.27}$$

Multiplying both sides of (3.37) by $\mathbf{R}^{-1}$, the inverse of the correlation matrix, we can find the solution for $\mathbf{w}_k$ which minimizes $J(\mathbf{w}_k)$, namely,

$$\mathbf{w}_{opt} = \mathbf{R}^{-1}\mathbf{P} \tag{3.28}$$

This solution gives the optimal array weight vector in the MMSE sense. Equation (3.27) is called the Wiener-Hopf equation [10]. The optimum weight vector $\mathbf{w}_{opt}$ in (3.28) is called the Wiener solution.

3.4.2 Least Mean Square (LMS) Solution

Rather than solving $\mathbf{w}_{opt} = \mathbf{R}^{-1}\mathbf{P}$ directly, adaptive techniques are often used with an iterative approach which provides an updated weight vector, $\mathbf{w}_k$, after each computation. Typically, these algorithms have a per-step complexity that is much lower than the direct solution of above formulation, and can also track non-stationary channels.

It is intuitively reasonable that successive corrections to the weight vector in the direction of the negative of the gradient vector should eventually lead to the minimum mean-squared error $J_{\min}$, where the weight vector assumes its optimum value $\mathbf{w}_{opt}$.

Let $\mathbf{w}(k)$ denote the value of the weight vector at time k, (i.e., the n^{th} iteration). According to the steepest descent method, the update value of the weight vector at time

$k+1$ is computed by using the simple recursive relation

$$\mathbf{w}(k+1) = \mathbf{w}(k) + \frac{1}{2}\mu[-\nabla(J(k))] \tag{3.29}$$

where μ is a positive constant which is referred to as the step-size and controls the convergence rate of the adaptation. Algorithms of this type, that use the gradient of the mean square error function to update the weight vector, are called Stochastic Gradient Techniques.

Exact calculation of the gradient, $\nabla J(w)$, is cumbersome and involves matrix inversions. Therefore, other adaptive algorithms that are more efficient have been developed. One example is the Least Mean Square Error (LMS) Algorithm [15].

Substituting (3.23) into (3.29), we have

$$\begin{aligned}\mathbf{w}(k+1) &= \mathbf{w}(k) - \mu[\mathbf{R}\mathbf{w}(k) - \mathbf{P}] \quad k = 0,1,2,.... \\ &= \mathbf{w}(k) - \mu E\left[\mathbf{x}(k)\mathbf{x}^H(k)\mathbf{w}(k) - \mathbf{x}(k)d^*(k)\right]\end{aligned} \tag{3.30}$$

If the expectation operator is removed from (3.30), we have

$$\begin{aligned}\mathbf{w}(k+1) &= \mathbf{w}(k) - \mu\mathbf{x}(k)(\mathbf{x}^H(k)\mathbf{w}(k) - d^*(k)) \\ &= \mathbf{w}(k) - \mu\mathbf{x}(k)e^*(k)\end{aligned} \tag{3.31}$$

where $e^*(k)$ is the instantaneous error between the array output and the desired response. This is called the Least Mean Square algorithm and is a widely used for adaptive arrays.

3.4.3 Simulation Results for a Noisy Channel

Here we demonstrate and analyze the performance of the adaptive arrays developed in Section 3.4.1. For the proposed Multi-Target Space-Time Receiver (MT-STR) for a WCDMA FDD downlink, simulation results are obtained using Matlab. The channel used in the simulation consists of three equally spaced base stations. The time-invariant channel used in the simulations is shown in Table 3-1. We next simulate the antenna array beamforming ability for a noisy channel.

Table 3-1: Time-invariant channel used in the simulations

Path		Azimuth	Coefficient	Delay(In Chips)
BS0	(0,0)	0^0	1	1
	(0,1)	60^0	0.5	2
Bs 1	(1,0)	75^0	1	4
	(1,1)	120^0	0.4	5
BS2	(2,0)	150^0	1	8
	(2,1)	270^0	0.3	9

As we know, both the LMS and MMSE approaches require knowledge or estimation of the desired spatial filter output. This is accomplished by periodically sending a training sequence known to both the transmitter and receivers.

In WCDMA systems, as described in Chapter 2, both downlink and uplink have a pilot signal which is transmitted at the same time as the data signal. In the downlink, the pilot signal is either transmitted continuously as a CPICH channel, or multiplexed into

the data stream as a pilot symbol, as illustrated in Figure 2-3, 2-4. These two approaches provide different benefits, namely, the continuously transmitted CPICH channel is immune to fast fading, while the multiplexed pilot symbol minimizes self-interference. The pilot signal can also be used as the reference signal for adaptive beamforming. In this thesis, we use the CPICH channel to get the optimum weight, because it is transmitted continuously and through the same fading channel as the data.

Figure 3-9 shows the simulation results of a multi-target space-time receiver with six antenna elements, for a noisy channel with SNR=-10dB. It can be seen that each antenna tracks and forms the beam pattern for the desired user.

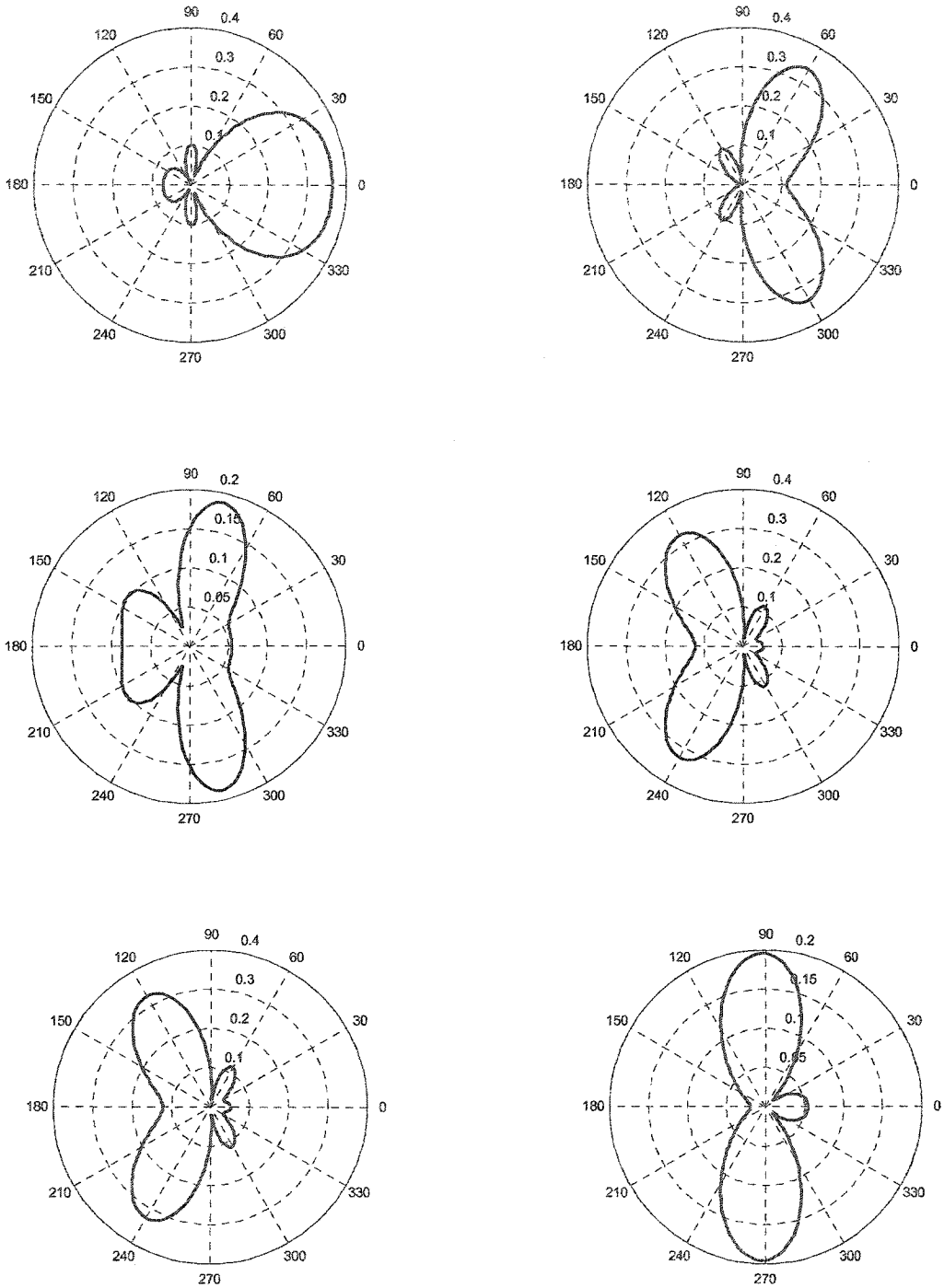

Figure 3-12: Beam pattern of 6-element LES antenna array with $d = 0.25\lambda$ and E_b/N_0 = -10dB

3.5 Summary

In this chapter, we have introduced terminology and basic concepts related to antenna arrays and adaptive beamforming, and discussed smart antenna technology and its performance. Using a WCDMA FDD system, we have first simulated a noise free receiver for the time-invariant channel model and analyzed the effects on the beam pattern (i.e., the spatial filtering ability) caused by different choices for the antenna array spacing d and the number of antenna array elements. We have found that increasing the number of elements in an antenna array or increasing the spacing between the array elements can improve the radiation pattern. We have also found that smaller spacing (such as 0.25λ) and a small number of elements can still provide a radiation pattern directed towards the desired user. At the end of this chapter, we have simulated the beam pattern using the presented adaptive algorithm for a noisy channel. Our simulation shows that the smart antenna is able to adaptively form a beam pattern directed towards the desired user.

Chapter 4

Performance Analysis of WCDMA Downlink Systems with Antenna Array

4.1 Introduction

In this chapter, we present a simulation study and performance analysis of a Space-Time Receiver (STR) structure that combines an antenna array with an adaptive temporal filter for WCDMA downlink systems. Under various conditions, we will simulate and evaluate the performance of the smart antenna system for the Third Generation (3G) WCDMA wireless communication handsets.

We first describe the WCDMA downlink transmission and receiving systems used in our simulation. We then simulate and analyze the dual antenna (i.e. an antenna array with two elements) downlink system for different channel conditions: Additive White Gaussian Noise (AWGN) and time-varying multipath fading channels. We evaluate the performance based on the resulting Bit Error Rate (BER). The simulation results for smart antenna handsets that use a diversity combining scheme are presented in Section 4.3 for both AWGN and multipath channels. The spatial-temporal receiver, which consists of 2 antennas and antenna processors, is presented in Section 4.4. We simulate

and analyze the performance improvement for both AWGN and multipath channels, resulting from the use of antenna array and adaptive combining.

4.2 WCDMA Downlink Systems

4.2.1 System Architecture and Major Operations

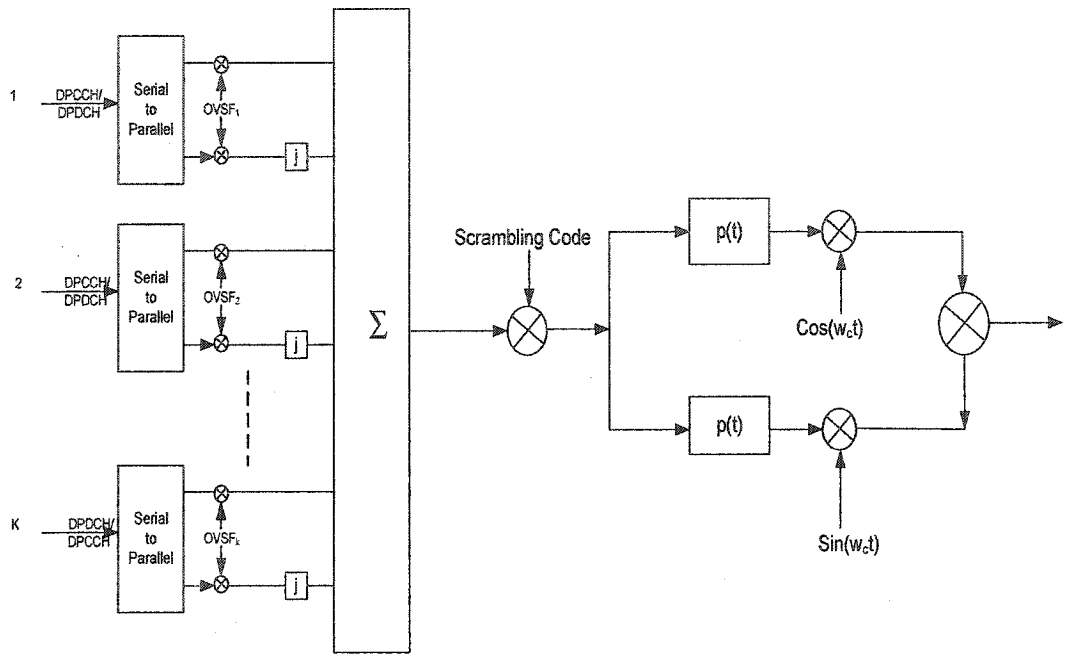

(a) WCDMA downlink transmission system

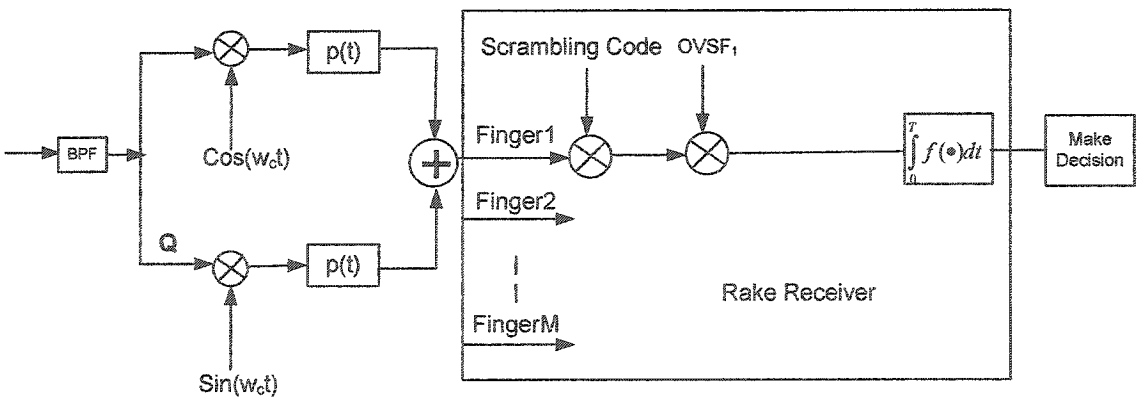

(b) WCDMA downlink receiving system

Figure 4-1: Block diagram of a WCDMA downlink system

Figures 4-1(a) and (b) show the block diagrams of WCDMA downlink transmission and receiving systems. In downlink transmission, a mobile receiver receives the signals of a number of simultaneously active users from a base station. The transmitted signal $s(t)$ with K users can be represented in the complex form as

$$s(t)=[a_0b_0(t)C_0(t)+a_1b_1(t)C_1(t)+\cdots+a_kb_k(t)C_K(t)]S_{dl}(t) \qquad (4.1)$$

where α_k, $b_k(t)$, and $C_k(t)$ represent the signal strength, the user data and the OVSF code for the k-th user (k = 1, 2, ..., K). $S_{dl}(t)$ is a scrambling code for the signal *s(t)*. Note that the first term in the right-hand side of (4.1) is for the common pilot channel (CPICH), in which $b_0(t)$ represents the fixed complex pilot symbol $(1+i)$ in QPSK format with $i=\sqrt{-1}$. The scrambled signal is then pulse-shaped by a square-root raised cosine filter with a roll-off factor of 0.22. The pulse shaped signal is subsequently upconverted to the carrier frequency.

Consider k users transmitting information from a base station through an AWGN channel. The received signal $r(t)$ at the mobile receiver can be represented by

$$r(t)=\sqrt{2S_m}S(t)+I(t)+n(t) \qquad (4.2)$$

where S_m is the average power of the received signal, *I(t)* the interference from adjacent cells, and *n(t)* the AWGN background noise.

In our simulation, we use dual receiving antennas. The input samples are received from the RF front-end circuitry in I and Q branches, and demodulated and pulse-shaped by a square root raised cosine filter with a = 0.2. The samples are then despread and

integrated using the spreading and scrambling codes of the desired user to recover the user data symbols; these operations are performed by the code generators and correlators.

4.2.2 Downlink Rake Receiver Structure and Channel Estimation

A block diagram of Rake receiver with three fingers and a single antenna is shown in Figure 4-2. Code generators and correlators perform the despreading and integration to recover the user's data symbol. The channel estimator uses the pilot channel for estimating the channel characteristics. The delay equalizer compensates for the difference in arrival times of the symbols in each finger. The Rake combiner then sums the channel-compensated symbols, thereby providing time diversity against the multipath fading.

Now consider k users transmitting information through a channel with M multipath components. The received input signal $r(t)$ from the RF front-end at the mobile receiver can be represented as

$$r(t)=\sum_{m=1}^{M}\sqrt{2S_m}\alpha_m(t)S(t-\tau_m)+I(t)+n(t) \tag{4.3}$$

where S_m is the average received signal power associated with the mth path, $\alpha_m(t)$ the complex channel coefficient of the m^{th} multipath component, τ_m the time delay of the m^{th} path, $I(t)$ the interference from adjacent cells, and $n(t)$ the background noise [35].

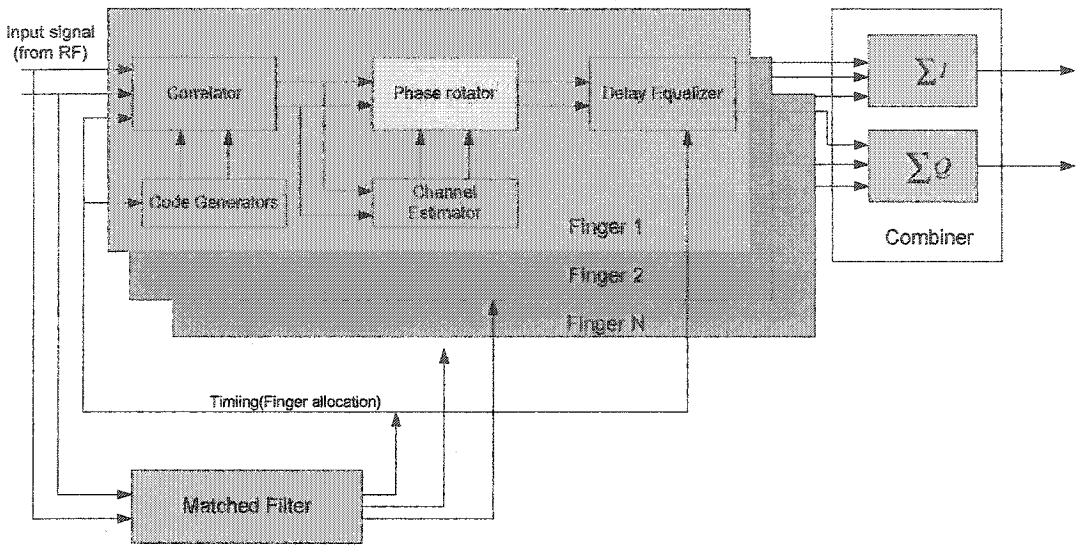

Figure 4-2: Block diagram of WCDMA RAKE receiver with single antenna

The RAKE receiver requires accurate estimates of the multipath channel delays and amplitudes. In Chapter 2, we have stated that pilot bits are included in the data structure of the physical channels in both downlink and uplink of WCDMA systems. Thus, WCDMA systems can use the pilot symbols (CPCCH) or common pilot channel (CPICH) to estimate the channel response, including the signal strength and phase. This information is used to coherently receive the signals; it can also be used for the adaptive antenna array. In the downlink, the common pilot signal (CPICH) is provided continuously from the base station to a mobile terminal. The channel estimator uses the pilot channel for estimating the channel response. In our simulation, we use the common pilot channel (CPICH) to perform channel estimation; the signal is multiplied by the channel coefficient estimated from the despread CPICH signal.

The RAKE combiner sums the channel-compensated symbols, thereby providing the time diversity against multipath fading. The coherent combining of multipath signals requires that each multipath signal be multiplied by the channel coefficient estimated from the despread CPICH signal. The pilot signal ($k = 0$) for the m[th] multipath is despread as shown below

$$\gamma_{0,m}(n) = \frac{1}{T_p} \int_{nT_p+\tau_m}^{(n+1)T_p+\tau_m} r(t)[S_{dl}(t-\tau_m)C_k(t-\tau_m)]^* d_t \tag{4.4}$$

where T_p is the pilot symbol period and n the symbol index. The k^{th} user signal (k = 1, 2... K) from the m[th] multipath is despread in the same manner as shown in (4.4) and is given by

$$\gamma_{k,m}(n) = \frac{1}{T_K} \int_{nT_K+\tau_m}^{(n+1)T_K+\tau_m} r(t)[S_{dl}(t-\tau_m)C_k(t-\tau_m)]^* d_t \tag{4.5}$$

where T_k is the data symbol period of the k[th] user. Then, the user signal from each multipath $\gamma_{k,m}(n)$ is coherently combined to produce an output signal as shown below

$$d_k(n) = \sum_{m=1}^{L} \gamma_{k,m}(n)\gamma_{o,m}{}^*(n) \tag{4.6}$$

where L is the number of RAKE fingers (which is equal to or smaller than the number of multipaths M).

4.3 System Simulation with Dual Antenna and Maximum Ratio Combining

4.3.1 Simulation for AWGN Channel

4.3.1.1 AWGN Channel

Additive noise is generated internally by components such as resistors and solid-state devices used to implement the communication system [16]. The AWGN noise added at the front end of the simulated receiver is generated by a Gaussian random number generator. The variance of the noise distribution depends on the SNR or E_b/N_0 at the front end of the receiver. The noise variance is also a function of the spreading factor, the signal amplitude, and the sampling rate or the number of samples per chip. The calibration of the noise is discussed as follows.

Figures 4-3 (a) and (b) show the chip and the double sided noise spectrum. Here, T_c is the chip duration, A is the chip amplitude, f_s is the sampling rate, N_0 is the noise power spectral density. Therefore, the energy per chip is

$$E_c = A^2 T_c \tag{4.7}$$

If the spreading factor is denoted as SF, then the energy per bit is

$$E_b = SF \cdot E_c = (SF) A^2 T_c \tag{4.8}$$

The noise variance is given by

$$\delta^2 = \frac{N_0 f_s}{2} \tag{4.9}$$

$$\frac{E_b}{N_0} = \frac{(SF)A^2 T_C}{2\delta^2 / f_s} = \frac{(SF)A^2 (T_C f_s)}{2\delta^2} \tag{4.10}$$

where $T_C f_s$ is equal to the number of samples per chip, m. As a result, we have

$$\frac{E_b}{N_0} = \frac{(SF)A^2 m}{2\delta^2}$$

$$\delta^2 = \frac{(SF)A^2 m}{2(E_b / N_0)} \tag{4.11}$$

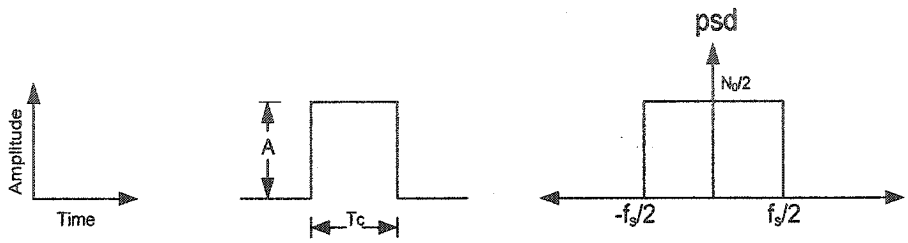

Figure 4.3(a) Chip

Figure 4-3(b): Noise Spectrum

Figure 4-3: Chip and double sided noise spectrum

4.3.1.2 Simulation Environment

In this section, we simulate a WCDMA transmission and receiving system on an AWGN channel. The system has dual receiving antennas on a handset. We compare single and dual antenna systems in terms of the BER performance. We also investigate the effects of different parameters (e.g., antenna spacing and number of users) on the performance of the dual antenna receiver.

The performance is evaluated with a link simulator in accordance with the WCDMA specification [31, 32, 33, and 34]. The information data are transmitted frame-by-frame

over an AWGN channel. An ideal delay estimation and finger allocation have been used. The AWGN noise has been calibrated according to (4.11), and is added at the front end of the RAKE receiver. In our simulation, we assume perfect power control so that all the signals arriving at the antenna array have the same power. The distance between two antenna elements is $\lambda/4$ (3.5 cm). Eight user signals with a spreading factor of 32, as well as the common pilot (CPICH) signal are channelized, combined, scrambled, pulse-shaped, and transmitted through the channel. Twenty percent of the total transmitted power is allocated to the CPICH; the remaining 80% is divided equally and allocated to each user signal. The interference of 8 users from adjacent cells is generated. The detailed parameters considered in this section are given in Table 4-1.

4.3.1.3 Simulation Results

The simulation results of the single and dual antenna systems are presented shown in Figure 4-4. The y-axis of a plot is the BER, and the x-axis is the ratio E_b/N_0. The upper graph in each plot is the BER of a Single Antenna (SA) system. The lower graph is the BER of the dual antenna system with MRC diversity combining scheme.

Table 4-1: Radio link parameters for system simulation

Items	Description	Parameter
1	Spreading code	OVSF
2	Spreading factor: SF-Data	32
3	Spreading factor: SF-CPICH	256
4	Data modulation	QPSK
5	Chip rate	3.84Mcps
6	Synchronization	Perfect
7	Number of users	8
8	Carrier frequency	2.14GHz
9	Power Control	Perfect
10	Square Root Raised Cosine shaping filter	a = 0.2
11	Error correction coding	No
12	Distance between the two antennas	0.25λ
13	Channel Estimation	Pilot assisted channel estimation (3-symbol average)

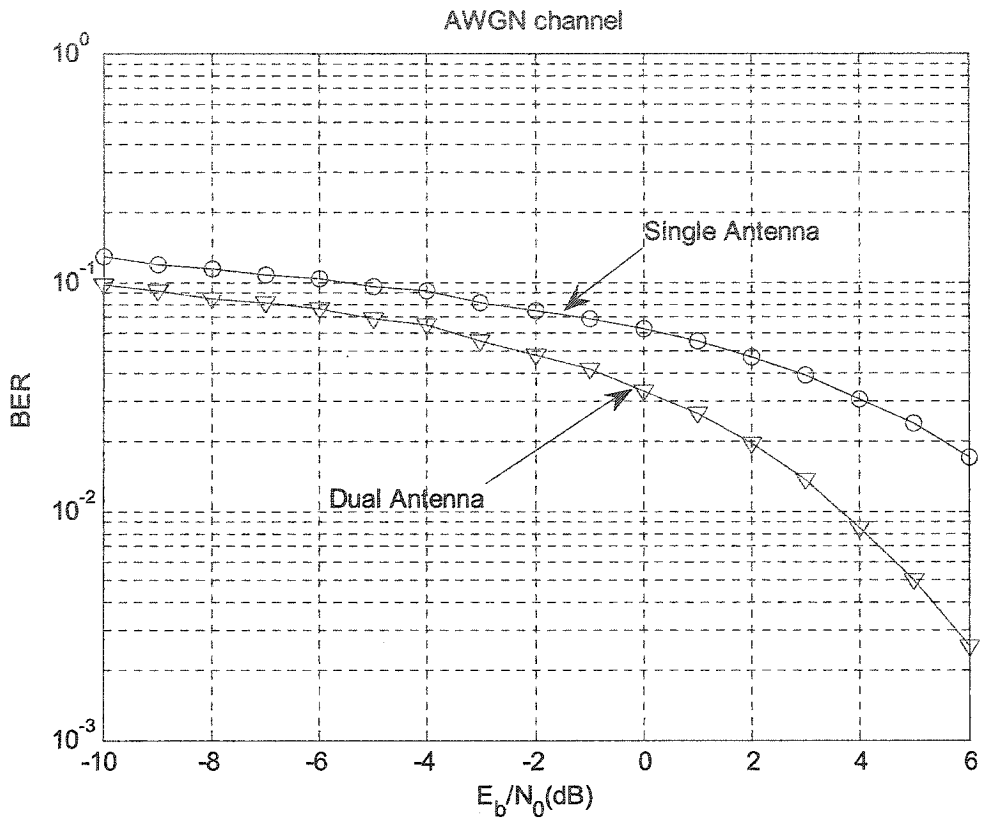

Figure 4-4: Performance of the dual antenna system with MRC combining method

From the figure, we can see that the dual antenna system always provides better performance than the single antenna system, and the performance gain increases further with respect to a relatively low BER. For example, for BER=9×10^{-2}, E_b/N_0 can be reduced by 3.6dB.

We next investigate the performance with different spacing distance d between the dual antenna elements. The simulation results with different antenna distances are presented in Figure 4-5. Note that all the other parameters are the same as in Table 4-1. The top curve represents the BER of a single antenna system; the remaining three curves represent the BER of the dual antenna system for antenna distances of $\lambda/8$, $\lambda/4$, and $\lambda/2$

respectively. From the curves, one can see that the dual antenna system achieves higher performance as the distance between the two antennas is increased. Considering the space limitations of mobile handsets, $\lambda/4$ (3.5 cm) appears to be the optimum antenna spacing for a dual antenna system for handsets. The detailed BER performance comparison is shown in Table 4-2.

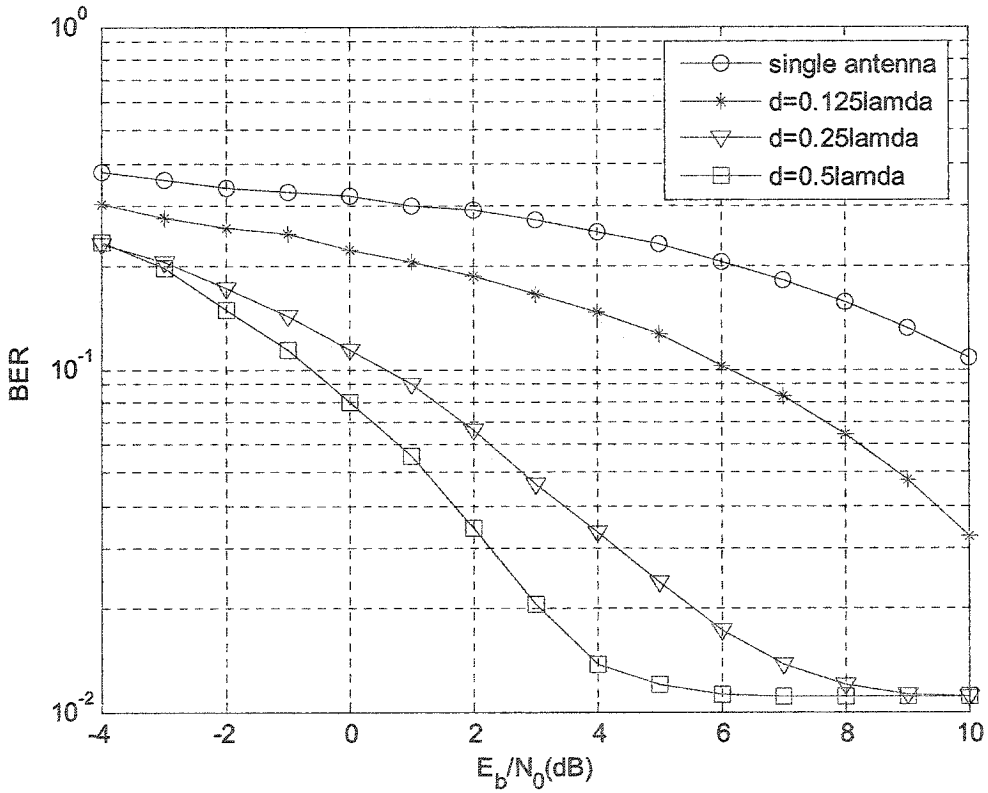

Figure 4-5: Performance improvement with different antenna distances

Table 4-2: BER performance comparison between single antenna and dual antenna of different distance d

E_b/N_o(dB) / BER / Distance	-2	0	2	4	6	8
Single Antenna	0.3387	0.3200	0.2903	0.2516	0.2063	0.1574
d = λ/8	0.2580	0.2234	0.1872	0.1469	0.1024	0.0642
d = λ/4	0.1727	0.1135	0.0664	0.0335	0.0172	0.0119
d = λ/2	0.1484	0.0799	0.3413	0.0138	0.0113	0.0110

We now investigate the BER performance improvement of the dual antenna system with different numbers of users transmitted via the same base-station, i.e. the effect of co-channel interference.

The simulation results are presented for 1, 8 and 24 users in Figure 4-6. Note that all the other parameters are the same as in the Table 4-1. The three dashed lines represent the BER performance of the single antenna system; the solid lines represent the BER of the dual antenna system. It is seen from these plots that the BER performance decreases as the number of users increases. This is because increasing the number of users decreases the relative signal power allocated to the desired user, resulting in an increase in the power level of the interference. However, with an increased number of users, the dual antenna system can provide more acceptable performance than a single antenna receiver; for

example, when E_b/N_o =12 dB and 24 users exist in the system, the dual antenna can provide BER=9×10^{-2}, but a single system can only yield BER=4×10^{-2};

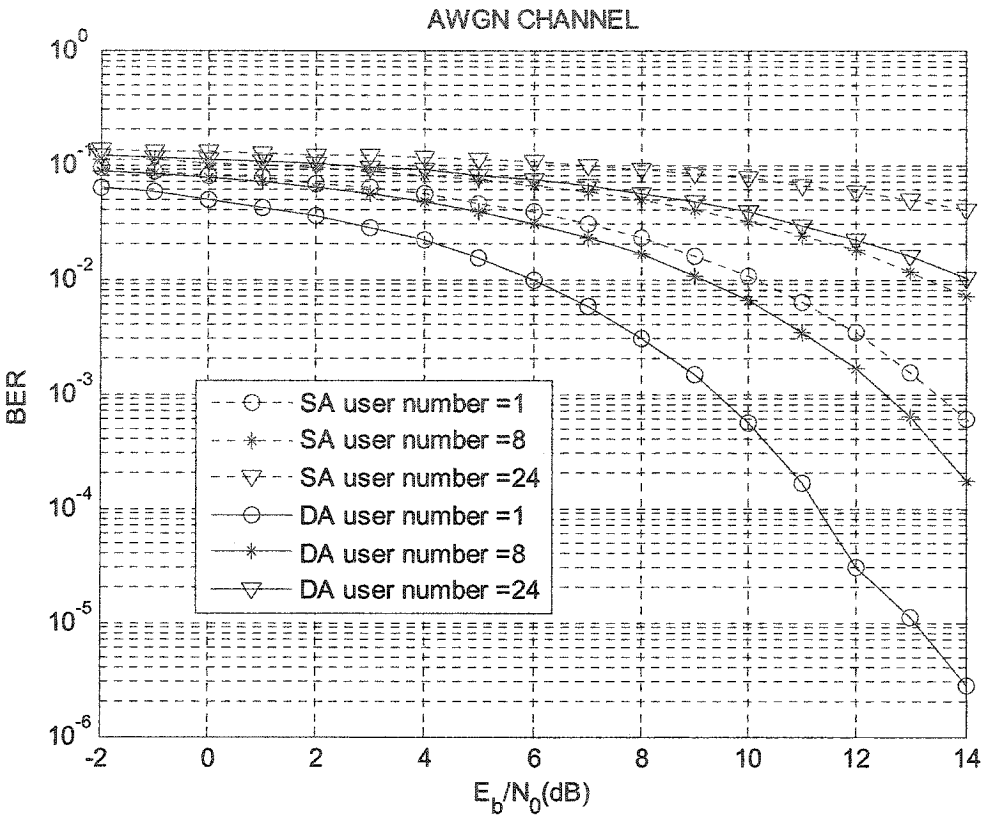

Figure 4-6: Performance comparison for different number of users

4.3.2 Simulation for Multipath Channel

4.3.2.1 Simulation Environment

The simulation environment is based on the fact that the power delay profile of a mobile radio environment may be resolved into a small number of multipaths having significant energy. The multipath fading channel model used in our simulation is shown in Figure 4-7 [4].

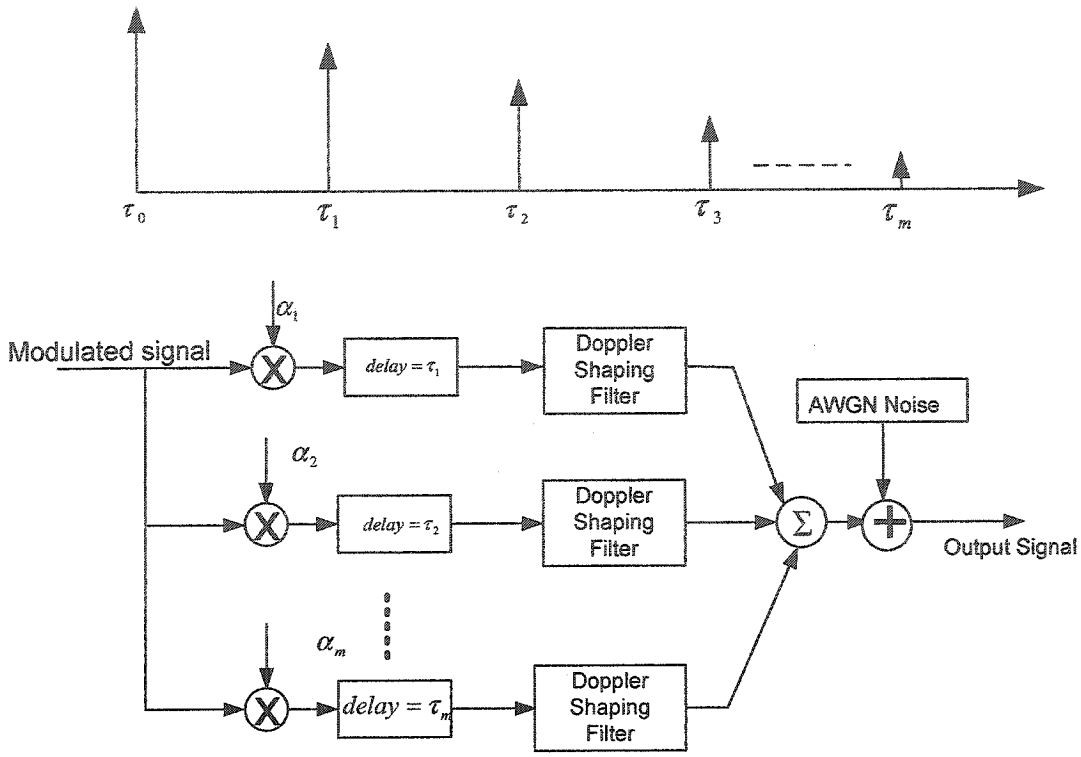

Figure 4-7: Time-varying multipath radio channel model

The signal on each path m is attenuated by α_m dB) and delayed by τ_m seconds. The first branch represents a direct path between the transmitter and receiver antennas. Due to the relative motion between the mobile and the base station, each multipath wave experiences an apparent shift in frequency; this shift in the received signal frequency due to motion is called the Doppler shift. We use Clarke's model to get the instantaneous value of the fading envelope with Rayleigh distribution, and also pass the delayed signal through a Doppler shaping filter. The frequency response of a Doppler shaping filter, shown in Figure 4-8, is designed to approximate the theoretical spectrum of the received signal envelope of (4.12). Signals from all branches are summed together and then combined with additive white Gaussian noise [17].

$$S_m(f) = \frac{k_c}{pf_m\sqrt{1-\left(\frac{f-f_c}{f_m}\right)^2}} \tag{4. 12}$$

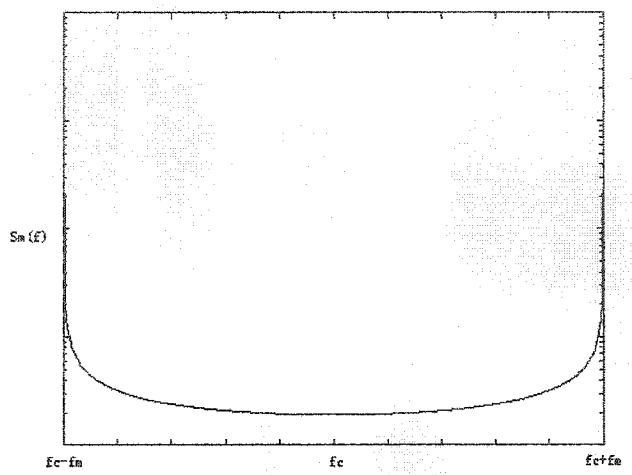

Figure 4-8: Spectral density of an RF signal with Doppler shift

It is clear that the Doppler shift is symmetric about the carrier frequency f_c, and the span of the spectrum is $2f_m$, where f_m is the maximum Doppler frequency,

$$f_m = v/\lambda = v\frac{f_c}{c} \tag{4. 13}$$

where v is the velocity of the mobile relative to the base station.

In our simulation, we have considered the following model parameters:

- A mobile velocity of 90 km/hr, which results in a maximum Doppler frequency of 178 Hz for a 2.14 GHz carrier frequency.
- Three multipath signals arriving at the handset antennas; each signal having the channel profile obtained from the Clarke's models; each path having a classic Doppler spectrum.
- At the handsets, a Rake receiver having three RAKE fingers.

- Ideal delay estimation and finger allocation.
- All other parameters in Table 4-1.

4.3.2.2 Simulation Results

In this subsection, we compare the BER performance of the single antenna system and that of the dual antenna system for multipath fading channels. We then investigate the performance improvement of the dual antenna systems for different numbers of paths.

The simulation results for the single and dual antenna systems with a velocity of 90km/hour for multipath channels are presented in Figure 4-9. The y-axis of a plot is the BER, and the x-axis is the ratio of the symbol energy of the first multipath signal to the AWGN. The upper graph is the BER of a Single Antenna (SA) system; the lower graph is the BER of the dual antenna system with MRC diversity combining scheme. From the figure, it is seen that the dual smart antenna system always provides better performance than a single antenna system, e.g., the performance gain is 8 dB at BER = 10^{-2}.

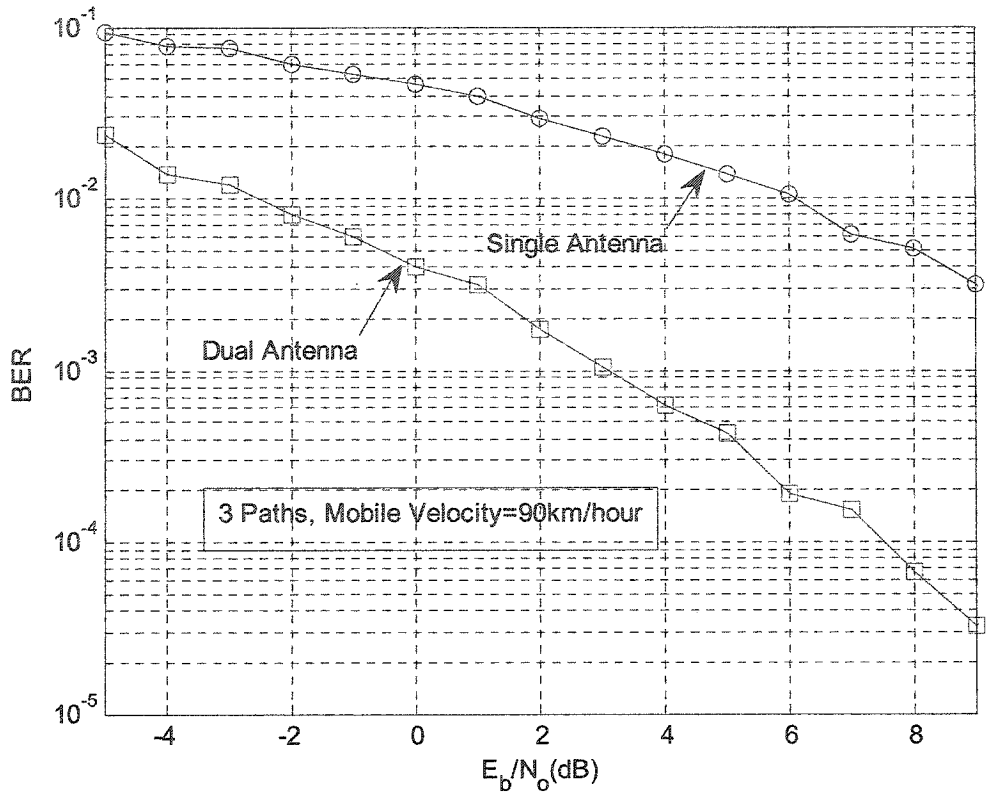

Figure 4-9: Performance with velocity of 90 km/hour

Next, we simulate the effect of varying the number of multipaths, while all the other parameters are kept the same as in Table 4-1. The simulation results are given in Figure 4-10 and Figure 4-11. Figure 4-10 presents the BER performance for a 2-paths environment; Figure 4-11 presents the BER performance for a 4-path environment. Comparing these simulation results, we found that more paths can give more diversity, and the dual smart antenna system performs much better than a single antenna system.

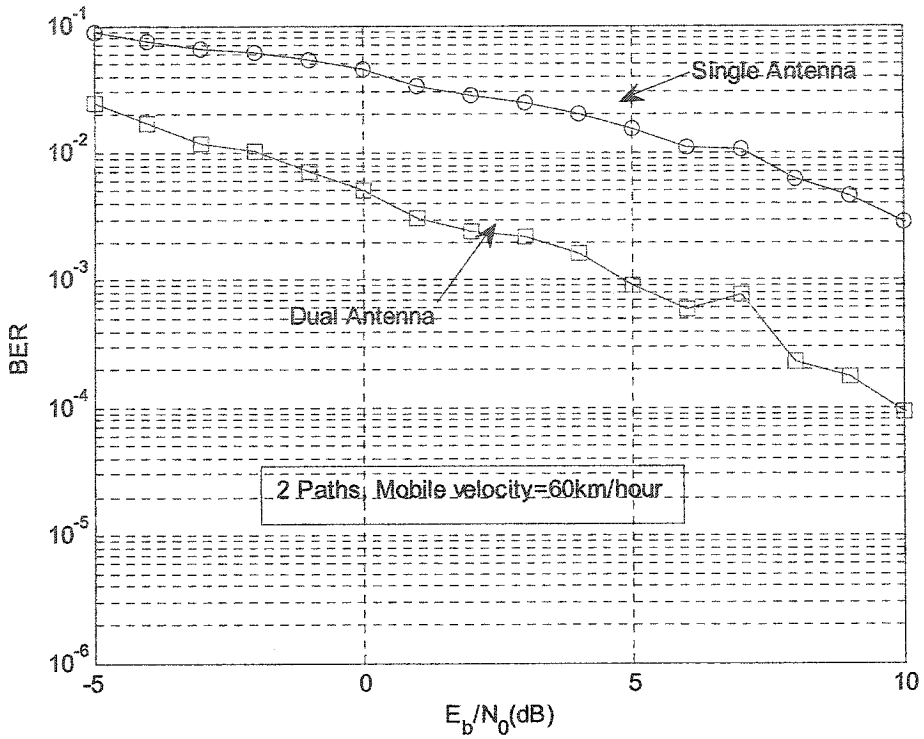

Figure 4-10: BER performance with 2 paths

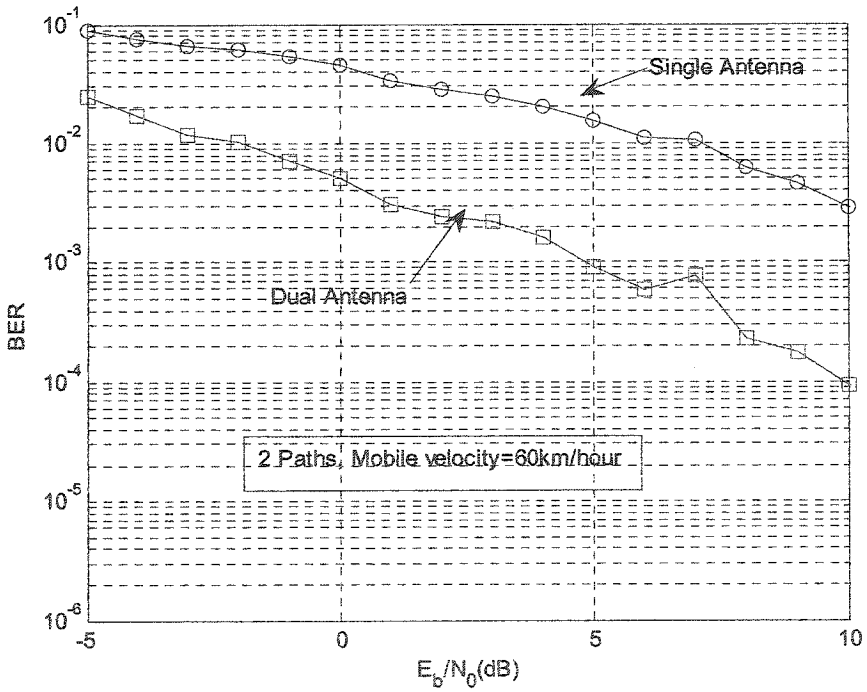

Figure 4-11: BER performance with 4 paths

4.4 System Simulation with Dual Antenna and Adaptive Combining

This section presents the results of a simulation to evaluate the performance of the dual smart antenna handsets with an adaptive combining scheme. This adaptive combiner combines the corresponding finger outputs of the two antennas with appropriate antenna weights, which are recursively obtained based on the N-LMS algorithm.

4.4.1 Adaptive Combining Method

In our simulation, we use dual receiving antennas in a mobile handset. Each antenna is followed by several RAKE fingers, so that the system can receive signals from all the multipaths. An antenna array receiver for a coherent WCDMA downlink is shown in Figure 4-12; only a single RAKE finger of one antenna is depicted. In WCDMA systems which experience frequency selective fading, multiple signals paths have to be coherently combined and one RAKE finger is required for each separable propagation path [35].

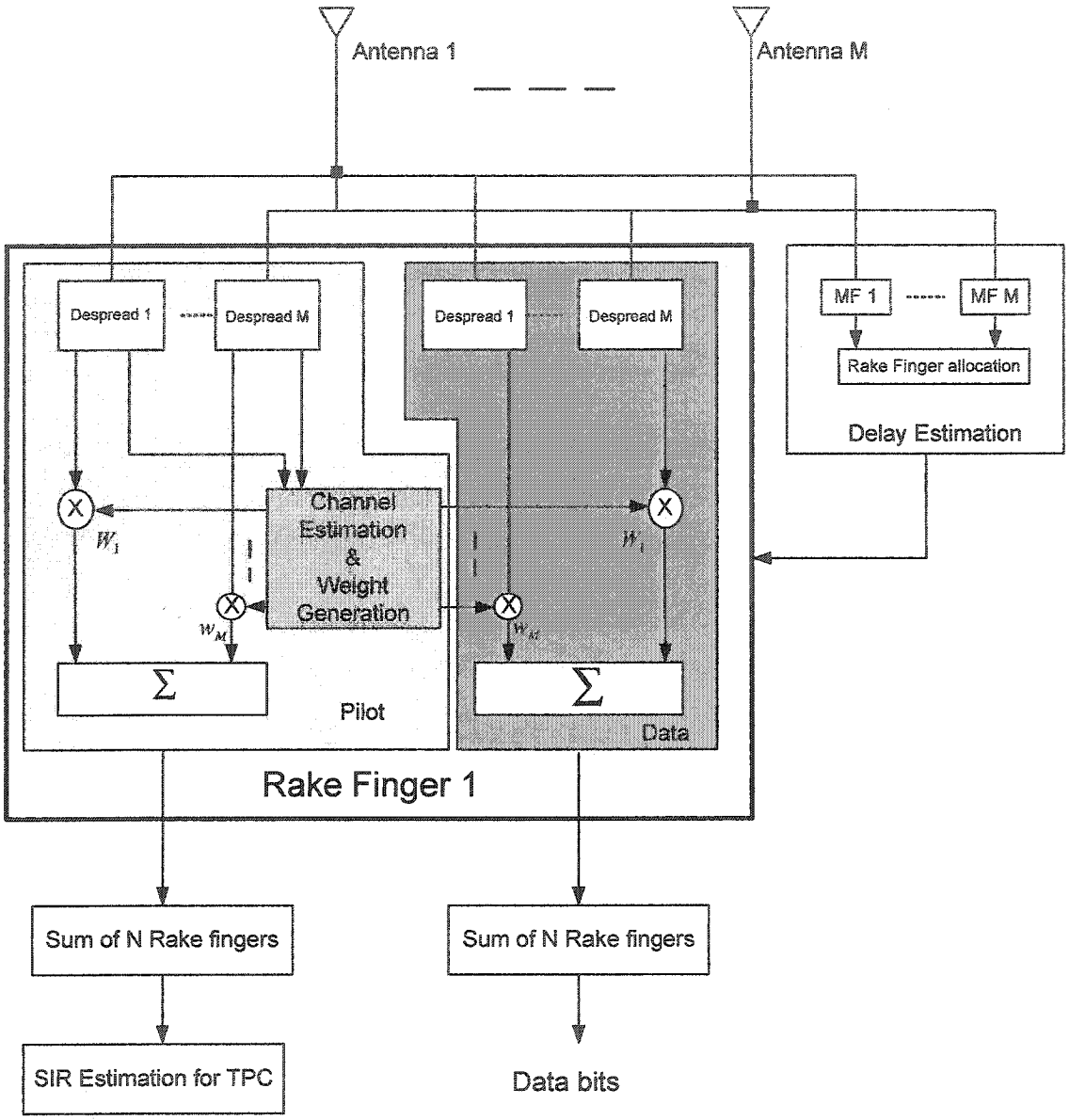

Figure 4-12: Antenna array receiver of WCDMA downlink system

The received signal with added background noise, is shaped back by a square root raised cosine filter with a = 0.22. Each Rake finger despreads a multipath signal from each antenna. There are two Rake finger outputs for each multipath signal: the despread pilot signal and the despread data signal. To combine each multipath signal from dual antennas, an adaptive combining scheme is applied. Figure 4-12 shows a dual antenna system with

the adaptive combining scheme; the despread signal from each antenna is weighted and combined. A filter is used for channel impulse response estimation, which is a Finite Impulse Response (FIR) filter with a length of P, where P is at least equal to the delay spread of the channel. When P input samples are read into the delay line of the filter, one output sample is produced. The output sample is an estimate of the transmitted multi-user symbol. To minimize the mean square error, the antenna weights are recursively obtained using the N-LMS algorithm described in Chapter 3.

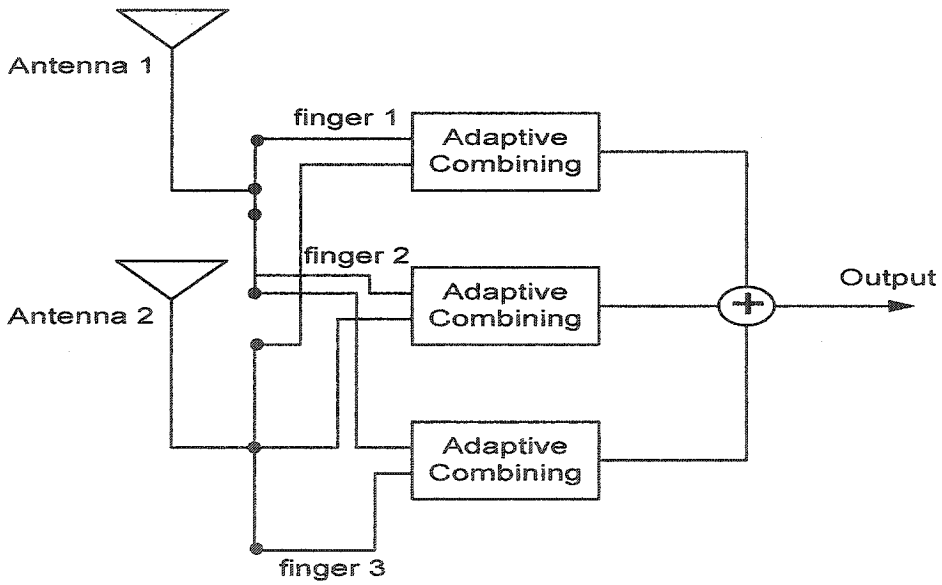

Figure 4-13: Adaptive combining of a dual antenna system

The procedure to obtain the antenna weights is explained below which is based on the adaptive combining algorithm presented in [40]. We have modified the algorithm and changed the 1 tap filter with a filter of a length of P element. The P-element input signal vector to the filter for the m^{th} multipath of the j^{th} antenna is denoted as

$$?_m^{(j)}(n) = (\gamma_m^{(j)}(n-P+1) \quad \cdots \quad \gamma_m^{(j)}(n-1) \quad \gamma_m^{(j)}(n))^T \tag{4.14}$$

The filter coefficient vector for the m^{th} multipath of the j^{th} antenna is given by

$$\mathbf{w}_m^{(j)}(n) = (w^{(j)}_{m,(P-1)} \quad \cdots \quad w^{(j)}_{m,2} \quad w^{(j)}_{m,1} \quad w^{(j)}_{m,0})^T \tag{4.15}$$

A new antenna weight $w_m^{(j)}(n+1)$ for the m^{th} multipath on the j^{th} antenna of the p^{th} tap is updated as follows [55].

$$w_{m,p}^{(j)}(n+1) = w_{m,p}^{(j)}(n) + \mu\gamma^{(j)}{}_{0,m}(n+1) / \sum_{j=1}^{2} \left|\gamma^{(j)}{}_{0,m}(n)\right|^2) e^*{}_{0,m}(n) \tag{4.16}$$

where $w_{m,p}^{(j)}(n)$ is the current antenna weight of the p^{th} tap of the filter, $\gamma^{(j)}{}_{0,m}(n)$ the despread pilot signal for the m^{th} multipath on the j^{th} antenna, μ the step size in the range of $0 < \mu < 2$, and $e_{0,m}(n)$ the error signal, which can be expressed as $\hat{d}_{0,m}(n) - d_{0,m}(n)$ where $\hat{d}_{0,m}(n)$ is the desired reference pilot signal for the m^{th} multipath signal and $d_{0,m}(n)$ is the combined pilot signal. We assume that the pilot signals from each antenna are ideally phase shifted and combined to obtain the desired reference pilot signal. Hence, the desired reference pilot signal $\hat{d}_{0,m}(n)$ is obtained by averaging the despread pilot signals, namely,

$$\hat{d}_{0,m}(n) = \frac{(1+i)}{\sqrt{2}} \frac{\sum_{l=0}^{Q-1} (\left|\gamma^{(1)}{}_{0,m}(n-1)\right| + \left|\gamma^{(2)}{}_{0,m}(n-1)\right|)}{Q} \tag{4.17}$$

where Q is the number of pilot symbols to be averaged and $(1+i)$ is the known transmitted pilot symbol. The combined pilot signal $d_{0,m}(n)$ for the m^{th} multipath is obtained using

the pilot signals $\gamma_{0,m}{}^{(j)}(n)$ from each antenna and the current antenna weights $w^{(j)}{}_{m,p}(n)$ such that

$$d_{0,m}(n) = \sum_{j=1}^{2} \sum_{p=0}^{P-1} \gamma^{(j)}{}_{0,m}(n-p) * w^{(j)}{}_{m,p}{}^{*}(n) \qquad (4.18)$$

After the antenna weights are obtained, the despread k^{th} user signal for the m^{th} multipath from each antenna is weighted and combined as

$$d_{k,m}(n) = \sum_{j=1}^{2} \sum_{p=0}^{P-1} \gamma^{(j)}{}_{k,m}(n-p) w^{(j)}{}_{m,p}{}^{*}(n) \qquad (4.19)$$

where $\gamma^{(j)}{}_{k,m}(n)$ is the despread k^{th} user signal for the m^{th} multipath on the j^{th} antenna and $w^{(j)}{}_{m,p}(n)$ is the obtained antenna weight. Then, the combined user signal from each multipath $d_{k,m}(n)$ is coherently combined to produce an output as shown below:

$$d_{k}(n) = \sum_{m=1}^{L} \gamma_{k,m}(n) \qquad (4.20)$$

where L is the number of RAKE fingers. The same antenna weight $w^{(j)}{}_{m}(n)$ is applied to obtain the successive user data symbols during the corresponding one pilot symbol.

4.4.2 Simulation Environment

Each antenna receives not only the transmitted signal from the desired base station but also the transmitted signals from adjacent base stations. Multiple Access Interference (MAI) is generated in a structured way rather than treating it as AWGN. The environment considered in the simulation is almost the same as in the Table 4-1.

4.4.3 Simulation Results

The simulation results for AWGN channel with adaptive combining are presented in Figure 4-14. In the figure, the y-axis is the BER and the x-axis is the ratio of the symbol energy of the first multipath signal to the AWGN. Note that all the other parameters remain the same as in the Table 4-1.

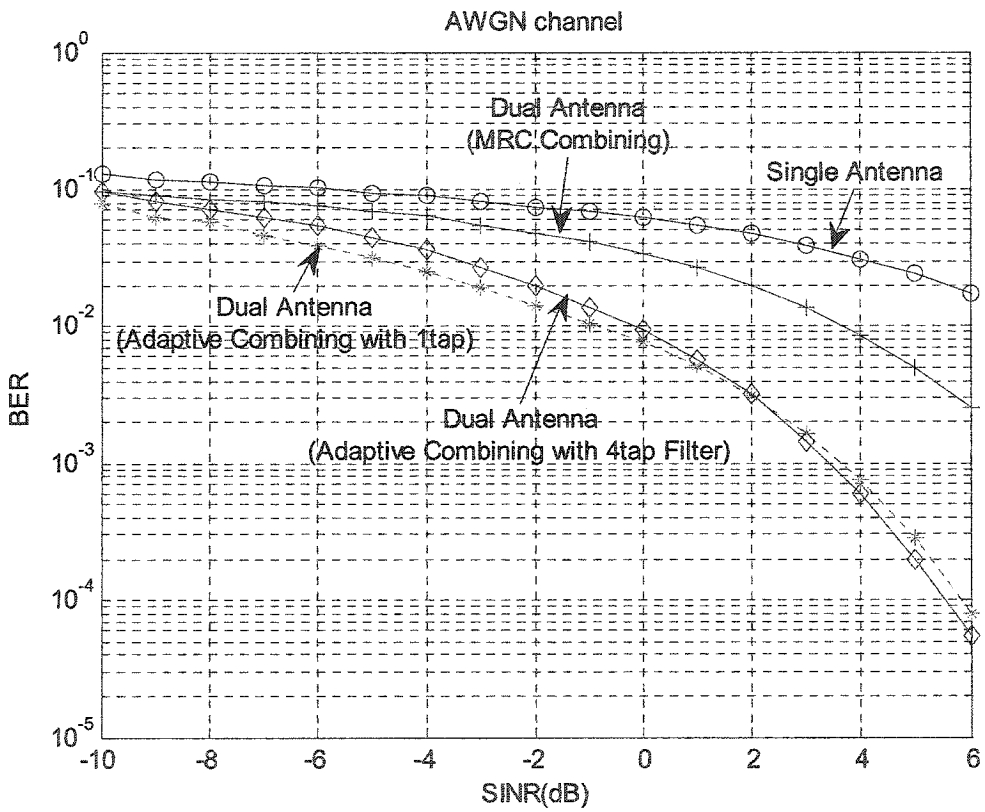

Figure 4-14: Performance improvement with adaptive combining for AWGN channel

The top line represents the BER of a single antenna system. The dashed line in the bottom represents the BER of a dual antenna system with adaptive combining algorithm presented in [40], and the solid line in the bottom represents the BER of a dual antenna system using the proposed adaptive combining algorithm. As can be seen from the figure,

the dual antenna system with adaptive combining performs better than either a single antenna system or the MRC space diversity combining method. The performance gain of the dual antenna system with the adaptive combining over a single antenna system when BER = $5x10^{-2}$ is 3.3 dB for the AWGN channel. The proposed algorithm gives a slight better performance improvement when the $E_b/N_o \geq 2$dB. At the beginning of the curve, we can see that the performance obtained using our algorithm is slightly worse than that using the algorithm presented in [40], for the reason that our proposed algorithm has more filter taps, implying a convergence rate. Again, the simulation results reveal that the dual antenna system performs better than a single antenna system.

The simulation results for multipath fading channel using adaptive combining when the mobile velocity is 90km/hour are presented in Figure 4-15. In the figure, the y-axis is the BER and the x-axis is the ratio of the symbol energy of the first multipath signal to the AWGN. Note that all the other parameters remain the same as in the Table 4-1.

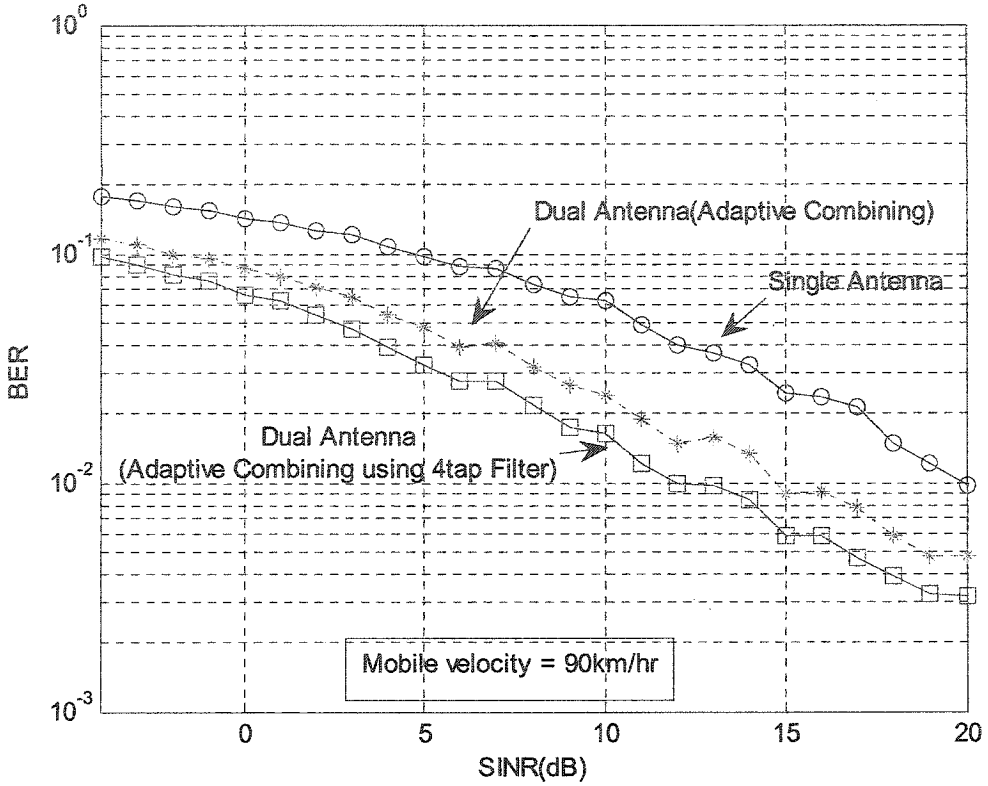

Figure 4-15: Performance improvement with adaptive combining for multipath channel

The top line represents the BER of a single antenna system. The dashed line in the bottom represents the BER of a dual antenna system with adaptive combining algorithm presented in [40], and the solid line in the bottom represents the BER of a dual antenna system using the proposed adaptive combining algorithm. As can be seen from the figure, the dual antenna system with adaptive combining performs better than a single antenna system. For a time-varying channel with both the Rayleigh distribution and the Doppler frequency shift, the proposed algorithm gives a better performance improvement than that using the algorithm presented in the literature; the reason is that our proposed method uses more filter taps and thus the channel variation can be better tracked. The E_b/N_o value of the

dual antenna system with the proposed algorithm can be reduced by 4 dB compared to that presented in the literature at the BER level of 9×10^{-2}.

4.5 Conclusions

In this chapter, we have presented the simulation results to evaluate the performance of the proposed dual antenna system for WCDMA mobile handsets in both AWGN and time-varying multipath fading channels.

We have found through computer simulations that a dual antenna with element spacing of $\lambda/4$ (i.e. 3.5cm) is practicable and provides significant performance improvement over a single antenna system. As the number of users increases, a dual antenna receiver provides more acceptable performance than a single antenna. For example, when $E_b/N_o = 7$ dB, dual antenna gives BER $=9\times10^{-2}$, but a single antenna only leads to BER $=5\times10^{-2}$. As the number of uncorrelated multipaths increases, a dual antenna receiver can make use of both the temporal and spatial diversity to provide better performance than a Rake receiver. Also, a dual antenna receiver with adaptive combining is able to provide a better performance under varying transmission channel conditions than a single antenna system.

Chapter 5

Conclusion and Future Work

5.1 Summary of the Work

Since the next-generation wireless communication systems aim to provide mobile users with high-speed multimedia services, the downlink data traffic will be much higher than the uplink channel. In this thesis, therefore, we have focused our research efforts on the downlink performance analysis. We have investigated the downlink performance of a WCDMA system using smart antenna technology. We have employed a Rake receiver to exploit the gain arising from temporal diversity, and used adaptive antennas at the receiver to take the advantage of the spatial diversity in multipath fading environments.

Considering the additional cost and complexity as well as the uncertainty in performance enhancement due to multiple antennas in the mobile terminal that have so far prevented antenna array from being utilized in the existing mobile communication systems, we have studied how employing multiple antennas in the WCDMA handset would improve the system performance. Based on the WCDMA specification, we have found that the spatial-temporal receiver of $\lambda/4$ (3.5cm) distance between the antenna elements could provide good beamforming capability. We have investigated the diversity gain of a smart

antenna system with different combining schemes. We have also shown that when spatial signal processing is combined with temporal signal processing, the interference and multipath fading effect can be well mitigated.

We have evaluated a smart antenna system used in mobile handsets for WCDMA FDD communication systems in which the two antennas are separated by a quarter wavelengths (3.5cm). We have implemented a signal simulator according to the physical layer specifications of the WCDMA FDD standard. In our simulation, data symbols are transmitted on a frame-by-frame basis through a time varying channel, the transmitted signal is corrupted by multiple access interference, and the signal is further corrupted by AWGN at the front end of the receiver. The smart antenna technique is combined with the Rake receiver at the receiving end. We have investigated the downlink channel BER performance for both AWGN and multippath fading channels. It has been shown from the simulation results that the performance can be improved significantly by using an antenna array with adaptive algorithms.

In a line-of-sight situation without fading, the optimal receiver is a beam former that performs antenna phasing of the LES antenna array in a way that sets the main beam to the direction of the desired signal. In the receiver in Figure 3-2, beam forming can be obtained by choosing the phase angles of antenna weights w_m so that the beam is adjusted to the direction that gives the largest desired signal power.

5.2 Suggestions for Future Study

The research work completed in this thesis leads naturally to some extensions which include but are not limited to the following.

In this thesis, we have used the most commonly used Clarks' multipath fading channel model. In future work, one could attempt some other channel models which pay more attention to the location of interference coming from other base-stations, to reveal the influence of the interference strength and the direction of angle.

The dual antenna approach for the mobile terminal can be expected to support the inter-frequency handover from or to other systems, including the GSM. Inter-frequency handover will be used to take care of high capacity needs in hot spots. Inter-frequency handover may also be needed for the second-generation systems, like GSM and IS-95. In order to complete inter-frequency handovers, an efficient method is needed for making measurements on other frequencies while still having the connection running at the current frequency.

The dual receiver approach is considered suitable in mobile terminals, especially when the mobile terminal employs antenna diversity for inter-frequency handover. The advantage of the dual receiver approach is that there is not break in the current frequency connection [15], [35]. In the future, one could also simulate and combine these functions together, which is very important for the WCDMA-GSM cooperating network.

References

[1] A. Mehrotha, *GSM System Engineering,* Norwood, MA: Artech House, 1997.

[2] B. Walke, *Mobile Radio Networks*, New York: Wiley, 1999.

[3] J. Korhonen, *Introduction to 3G Mobile Communications*, Norwood, MA: Artech House, 2002.

[4] H. Holma, and A. Toskala, *WCDMA for UMTS: Radio Access for Third Generation Mobile Communications,* John Wiley & Sons, 2000.

[5] G. Mandyam & J. Lai *Third Generation CDMA system,* Academic Press,2002

[6] F. Adachi, M. Sawahashi, and H. Suda, "Wideband DS-CDMA for next-generation mobile communication systems", *IEEE Communications Magazine*, Vol.36, No.9, pp. 56-69, Sept. 1998.

[7] http://www. itu.int

[8] http://www.umts-forum.org/

[9] A. J. Paulraj, and B. C. Ng, "Space time modems for wireless personal communications" *IEEE Personal Communications*, pp.36-48, February, 1998.

[10] R. Kohno, "Spatial and temporal communication theory using adaptive antenna array", *IEEE Personal Communications*, pp.28-35, February, 1998.

[11] J. H. Winters, "Smart antennas for wireless systems", *IEEE Personal Communications*, pp.23-27, February, 1998.

[12] B. Suard, A. Naguib, G. Xu, and A. Paulraj, "Performance analysis of CDMA

mobile communication system using antenna arrays", *Proc. ICASSP'93*, Vol. VI, Minneapolis, MN, pp. 153-156, April 1993.

[13] L. C. Godara, "Applications of antenna arrays to mobile communications, part I: performance improvement, feasibility and system considerations", *Proceedings of the IEEE*, Vol.85. No. 7, pp. 1031-1060, July 1997.

[14] L. C. Godara, "Applications of antenna arrays to mobile communications, part II: beam-forming and direction-of-arrival considerations", *Proceedings of the IEEE*, Vol.85. No.8, pp. 1195-1245, August 1997.

[15] J. C. Liberti, and T. S. Rappaport, *Smart Antennas for Wireless Communications: IS-95 and Third Generation CDMA Applications,* Prentice Hall, New Jersey, 1999.

[16] J. G. Proakis, *Digital Communications,* McGraw-Hill, U.S.A, 1998.

[17] T. S. Rapport, *Wireless Communications*, Prentice Hall, Upper Saddle River, New Jersey, 2002.

[18] J. S. Thompson, P. M. Grant, and B. Mulgrew, "Smart antenna arrays for CDMA systems", *IEEE Personal Communications*, pp. 16-25, October 1996.

[19] S. Tanaka, A. Harada, M. Sawahashi, and F. Adachi, "Experiment on coherent adaptive antenna array for wideband DS-CDMA mobile radio", *Electronics Letters,* Vol.34, No:23 pp.2204 – 2205, Nov. 1998

[20] J. Ramos, M.D. Zoltowski, and H. Liu; "A low-complexity space-time RAKE receiver for DS-CDMA communications", *Signal Processing Letters,* IEEE, Vol.4, No: 9, pp. 262-265, Sept. 1997.

[21] M. Dell'Anna, and A. H. Aghvami, "Performance of optimum and suboptimum combining at the antenna array of a WCDMA systems", *IEEE Journal on Selected Areas in Communications*, Vol. 17, No. 12, pp. 2123-2137, December, 1999.

[22] J. H. Winters, C. C. Martin, and T. Zhuang, "A two element adaptive antenna array for IS-136 base stations", *IEEE Communications Letters*, Vol. 3, No.3, pp. 60-62, March 1999.

[23] C. H. Gowda, V. Annampedu, and R. Viswanathan, "Diversity combining in antenna base station receiver for DS/CDMA system", *IEEE Communications Letters*, Vol. 2, No.7, pp.180-182, July 1998.

[24] C. B. Dietrich, K. Dietze, J. R. Nealy, and W. L. Stutzman, "Spatial polarization, and pattern diversity for wireless handheld terminals", *IEEE Transactions on Antennas and Propagation*, Vol. 49, No. 9, pp. 1271-1281, September 2001.

[25] M. Eseanin, and P. A. Ranla, "Interference rejection with a small antenna array at the mobile scattering environment", *In Proceedings of First IEEE Signal Processing Workshop on Signal Processing Advances in Wireless Commun. (SPAWC)*, La Bastille, Paris, April, 16-18th, 1997.

[26] P. B. Wong, and D. C. Cox, "Performance study of an adaptive dual antenna handset for indoor communications", *IEE Proceedings of Microwaves, antennas and Propagation*, Vol. 146, No. 2, pp. 138-1444, April 1999.

[27] http://www.3gpp.org/.

[28] B. O'Hara, and A. Petrick, *The IEEE 802.11 Handbook: A designer's Companion,*

IEEE Press, New Jersey, 1999.

[29] C. Bmun, M.Nilsson, R.D. Mush, "Measurement of the interference rejection capability of smart antennas on mobile telephones", *In Proceedings of Vehicular Technology Conference (VTC'99)*, Vol.2, pp. 1068-1073.

[30] G. F. Pedersen, and S. Skjaenis, "Influence on antenna diversity for a handheld phone by the presence of a person", *In Proceedings of Vehicular Technology Conference (VTC'97)*

[31] 3GPP TS 25.211 "*Physical channels and mapping of transport channels onto physical channels*", v3.3.0 June 2000

[32] 3GPP TS 25.212 "*Multiplexing and channel coding*", v3.3.0 June 2000

[33] 3GPP TS 25.213 "*Spreading and modulation*", v3.3.0 June 2000

[34] 3GPP TS 25.214 "*Physical layer procedures*", v3.3.0 June 2000

[35] L. Jaana, W.Achim, and N. Tomás, *Radio Network Planning and Optimisation for UMTS* , New York, Wiley, c2002

[36] M. B. Kundsen, B. N. Veligaard, and G. F. Pdersm, "Investigation of two branch transmit diversity with two branch receiver diversity", *IEEE VTC* 2000 Fall Conf. Record, Vol.5

[37] M. B. Kundsen, T. Baumgartner, and G. F. Pdersm, "Antenna system for interference reduction in a mobile handset", *IEEE VTC* 2000 Spring Conf. Record, Vol.2

[38] Z. Rong, and T. S. Rappaport, "Simulation of multi-target adaptive array algorithms

for wireless CDMA systems", *Proc. IEEE Vehicular Technology Conf.*, Apr. 1996.

[39] Z. Rong, "Simulation of Adaptive Array Algorithm for CDMA Systems", Master's Thesis MPRG-TR-96-31, Mobile & Portable Radio Research Group, Virginia Tech, Blackburg, VA, Sept.1996

[40] S. W. Kim, D. S. Ha, J. Ho Kim, and J. Hwan Kim, "Performance of smart antennas with adaptive combining at handsets for the 3GPP W-CDMA system" *IEEE VTC Fall Conference*, Vol.4, pp. 2048-2052, October, 2001

[41] M. Ventola, E. Tuomaala, and P. A. Ranta, "Performance of dual antenna diversity reception in WCDMA terminals" *IEEE VTC Spring Conference*, Vol.2, pp. 1035-1040, April, 2003.

[42] F.A.C.M. Cardoso, M.A.C. Fernandes, and D.S. Arantes, "Space-time processing for smart antennas in advanced receivers for the user terminal in 3G WCDMA systems" *IEEE Transactions on Consumer Electronics*, Vol. 48 , Nov. 2002 pp.1082- 1090

[43] F. Ling, "Pilot assisted coherent DS-CDMA reverse link communications with optimal robust channel estimation", *IEEE International Conference on Acoustics, Speech, and Signal Processing*, Vol.1, pp.263 - 266 Apr. 1997.

[44] S. Haykin, *Adaptive Filter Theory,* Prentice Hall, Upper saddle River, New Jersey, 2002.

[45] A. J. Viterbi, *CDMA Principles of Spread Spectrum Communication,* Addison Wsley, 1995.

[46] K. Petri and H. Ville, "Adaptive filtering for fading channel estimation in WCDMA downlink", *The 11th IEEE International Symposium on Indoor and Mobile Radio Communications*, Vol.1, pp.549-553, Sept. 2000.

[47] J. W. Choi and Y. H. Lee, "An adaptive channel estimator in pilot channel based DS-CDMA system", *The 55th IEEE Vehicular Technology Conference*, Vol.3, pp.1429-1433, May 2002.

[48] L. Lindbom, M. Sternad, and A. Ahlen, "Tracking of time-varying mobile radio channels—part I: the Wiener LMS algorithm", *IEEE Transactions on Communications*, Vol. 49, No. 12, pp.2207-2217, Dec., 2001.

[49] V. P. Kaasila, and A. Mammela, "Bit-error probability for an adaptive diversity receiver in a Rayleigh-fading channel", *IEEE Transactions on Communications*, Vol. 46, No. 9, pp. 1106-1108, Sept.1998.

[50] K. Wesolowski, C. M. Zhao, and W. Rupprecht, "Adaptive LMS transversal filters with controlled length", *IEE Proceedings on Radar and Signal Processing*, Vol.139, pp.233-238, Jun. 1992.

[51] A. Zhuang, and R. Markku, "Combined pilot aided and decision directed channel estimation for the Rake receiver", *The 52nd IEEE Vehicular Technology Conference*, Vol. 2, pp.710-713, Sept. 2000.

[52] H. Andoh, M. Sawahashi, and F. Adachi, "Channel estimation filter using time-multiplexed pilot channel for coherent Rake combing in DS-CDMA mobile radio", *IEICE Transactions on communications*, Vol. E81-B, No. 7, pp.1517-1525,

Jul. 1998.

[53] J. K. cavers, "An analysis of pilot symbol assisted modulation for Rayleigh fading channels", *IEEE Transactions on Vehicular Technique*, Vol.40, No.4, pp.689-693, Nov. 1993.

[54] Y. Honda, and K. Jamal, "Channel estimation based on time-multiplexed pilot symbols", *IEICE Technical Report*, RCS96-70, Aug. 1996.